# CHAPTER 1

# MOLECULAR CLIPS AND TWEEZERS WITH CORANNULENE PINCERS

ANDRZEJ SYGULA and WILLARD E. COLLIER



## 1-1. INTRODUCTION

Molecular receptors have long intrigued researchers, and many structural motifs have been synthesized. Chen and Whitlock, in 1978, described molecular tweezers designed to selectively bind planar π-conjugated molecules (Figure 1-1).[1] They listed three characteristics molecular tweezers needed in order to enhance complexation: (1) a rigid bridge or spacer preventing self-association of the arms or pincers, (2) a pincer-to-pincer distance sufficient for insertion of the "tweezed" molecule, and (3) a *syn* geometry of the pincers. Chen and Whitlock called attention to the rigid tweezerlike structure of echinomycin, a potent antineoplastic and antibiotic that intercalates into DNA, decades before the design of molecular clips for DNA.

Since 1978, numerous molecular tweezers have been synthesized[2] along with more recent structures termed *molecular clips*.[3] Logically, tweezers require a force to close onto the target molecule and will release the target when the applied force is released. In contrast, clips require a force to open and then, when the force is removed, the clip will close onto the target; thus clips likewise require a force to open and release the target. Several groups are working on dynamic molecular tweezers,[4] but as Harmata has noted, there is currently little difference between molecular clips and tweezers.[5] The distinction between clips and tweezers may soon be realized as more sophisticated structures are synthesized, but for now Harmata's observation remains valid.

Molecular tweezers and clips have the basic design illustrated above: a rigid spacer separating two pincers. Until relatively recently, all the molecular tweezers and clips designed to complex π-conjugated systems have incorporated planar pincers. But are all π-conjugated molecules planar? Why not design molecular clips and tweezers with curved pincers? That might seem a simple task. In reality, molecular clips and

*Fragments of Fullerenes and Carbon Nanotubes: Designed Synthesis, Unusual Reactions, and Coordination Chemistry*, First Edition. Edited by Marina A. Petrukhina and Lawrence T. Scott.

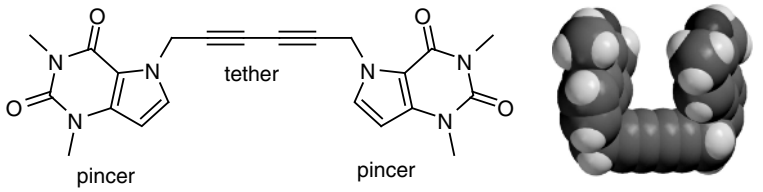


**Figure 1-1.** Chen and Whitlock's molecular tweezers. One of the possible conformations is shown.

tweezers with bowl-shaped pincers resulted from the convergence of a chance discovery that earned a Noble Prize and a 50-year quest to improve synthetic methodologies for a simple molecule. This account chronicles one of the author's contributions to the latter and their synthesis of the first buckycatcher.

### 1-1-1. PAHs: To Curve or Not to Curve?

A planar or near-planar geometry of carbon-based molecular networks is often cited as necessary for the efficient conjugation of π-electronic systems. However, it turns out that since the energy required for modest bending or twisting of polycyclic aromatic hydrocarbons (PAHs) is quite low, the crystal structures of several PAHs show severe distortion from planarity. For example, numerous significantly twisted PAHs retaining their conjugation have been synthesized and characterized,[6] including "the most highly twisted PAH ever prepared" (**1**) with an end-to-end twist of 144° (Figure 1-2).[7] The nonplanarity of **1** and related PAHs is induced by the steric repulsion of substituents (including hydrogen atoms) on the rim of the conjugated core.

In 1966, Barth and Lawton reported the first synthesis of a $C_{20}H_{10}$ hydrocarbon that they named *corannulene* (**2**).[8] This highly nonplanar PAH consists of five benzene rings arranged around the central five-membered "hub" ring and introduces a novel structural motif with two nonequivalent faces of the carbon network: *concave* and *convex* (Figure 1-3). In contrast to the previously mentioned twisted PAHs, the curvature of corannulene is not caused by bulky substituents but instead is a

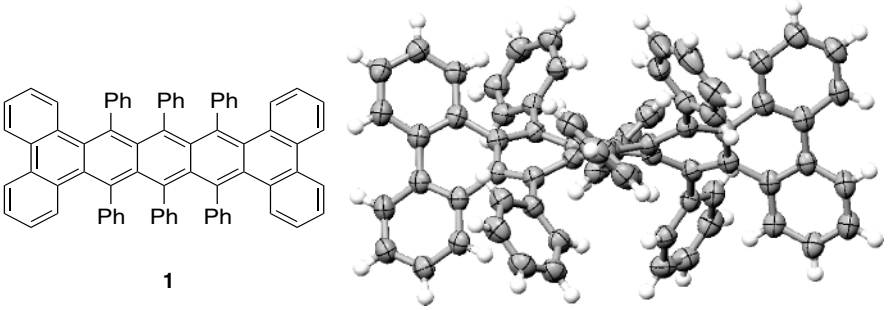


**1**

**Figure 1-2.** Pascal's " most highly twisted PAH ever prepared."

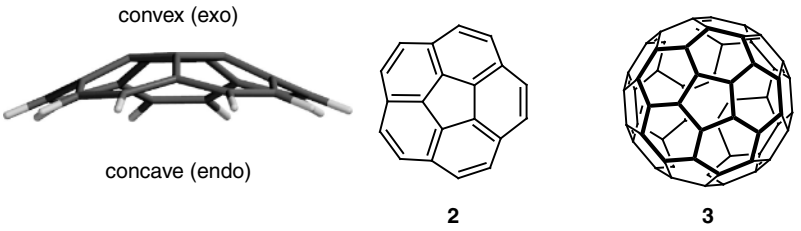


**Figure 1-3.** Corannulene and its structural relationship with fullerene $C_{60}$.

consequence of the incompatibility of abutting pentagons and hexagons in the construction of a planar sheet. Such a combination must result in formation of bowl-shaped surfaces and, in accord with Euler's theorem, if the number of pentagons reaches 12, a closed surface can be created.

In the mid-1980s, fullerenes, a new allotropic form of carbon, were discovered and earned Kroto, Curl, and Smalley a Noble Prize in 1996.[9] Icosahedral $C_{60}$ (**3**), commonly called *buckminsterfullerene* (after R. Buckminster Fuller, 1895–1983, American engineer), is the most studied member of the fullerene family. This nanoscale cage of $sp^2$-hybridized carbon atoms is constructed from six-membered rings along with 12 five-membered rings. Consequently, the corannulene carbon network is amply represented on the surfaces of fullerenes (Figure 1-3). This structural relation renewed interest in corannulene and related curved-surface PAHs, known as "buckybowls" or *fullerene fragments*.[10] There are numerous reasons for studying buckybowls. These bowl-shaped hydrocarbons may serve as models for fullerenes; they are potential precursors for rational syntheses of carbon cages, and, because of the complementary character of the carbon surfaces of buckybowls and fullerenes, there is a potential for host–guest supramolecular chemistry for these systems. An obvious but important observation is that buckybowls offer accessibility to both their convex and concave surfaces, in contrast to fullerenes, which possess an accessible convex surface only.

In this chapter, we will review more recent progress in the synthetic methodologies for buckybowls. These synthetic schemes have generated buckybowls in sufficient quantities to allow their incorporation into larger molecular architectures. We will then review novel synthetic methodologies for the construction of molecular clips and tweezers incorporating buckybowls as pincers. Finally, we will also discuss the potential of these structures to act as molecular clips and tweezers for the guest fullerene cages.

Since supramolecular tweezer–fullerene complexes depend on π–π interactions for molecular recognition, we first briefly review the performance of computational models in description of π–π interactions between conjugated carbon networks. Theoretical predictions of the binding potential of new molecular tweezers and clips will play an increasingly important role in identifying target molecules with desired complexation ability.[11] Therefore, we will examine the available experimental data from synthesized molecular clips and tweezers to assess the reliability of the theoretical models. Understanding the limitations and range of applicability of

theoretical methods is imperative if these methods are to guide the synthesis of large molecular tweezers.

## 1-2. π–π INTERACTIONS IN CURVED SURFACE SYSTEMS

### 1-2-1. π–π Stacking: Is It Important?

Planar aromatic molecules have long intrigued both experimental and theoretical chemists. The π–π interactions between various aromatic molecules are especially interesting. The benzene dimer has been scrutinized both experimentally and theoretically as the simplest model of π–π interactions. Despite its small size, 12 carbon and 12 hydrogen atoms, the benzene dimer is computationally challenging when investigators attempt to use the highest levels of theory {e.g., coupled cluster or quadratic configuration interaction method using single, double and perturbative triple excitations [CCSD(T) or QCISD(T)] with large basis sets} to predict chemically accurate properties.[12] Experimentalists and theoreticians are still not in complete agreement on the structure of the most stable complexes formed by the archetypal aromatic molecule, benzene.[13]

Once corannulene was synthesized and the concept of a curved aromatic surface became accepted, it was natural to ask questions about the strengths and types of interactions between bowl-shaped PAHs. The common packing motifs for planar PAHs are "herringbone" (characterized by edge-to-face interactions) and π–π stacking. The X-ray crystallography data for corannulene revealed no long-range stacking order.[14] In contrast, the crystal structure of cyclopentacorannulene, the second buckybowl ever synthesized, exhibited a stacked geometry.[15] Since then several other buckybowls have been synthesized, and the X-ray crystal data have revealed that π–π stacking is a common but not a general feature of the solid state of buckybowls.

The discovery of fullerenes prompted the vision of buckybowl–fullerene complexes since the concave buckybowl face nicely fits the convex fullerene surface. Although mass spectral data revealed the existence of corannulene–fullerene radical cation complexes in the gas phase,[16] no evidence exists for the presence of the neutral complexes in the condensed phases. Some pentakis- and decakis-substituted corannulenes with different arylthioether arms were synthesized and screened by NMR titration experiments for the formation of the substituted corannulene–fullerene complex in solution.[17] Moderate association constants with $C_{60}$ in the range of 60–1400 $M^{-1}$ were reported, confirming some complexation occurring in toluene solutions. While intriguing, these experiments did not prove the existence of strong π–π interactions between corannulenes and fullerenes. The reported association constants were relatively low and strongly substituent-dependent, so it can be argued that the rim substituent–fullerene interactions account for most of the binding, not π–π interactions between the bowl and the fullerene. The early investigations indicating that the interactions between corannulene and fullerene were not as strong as expected led to the conclusion that "the attractive force of the concave–convex π–π interaction is not so significant, if at all."[18]

The first definitive evidence for large π–π interactions between corannulene and $C_{60}$ was published in 2007, when we described the synthesis of a molecular tweezers with corannulene pincers, dubbed the "buckycatcher."[19] The buckycatcher is shown to have strong π–π interactions with the fullerene guest both in solution and in the solid state. X-ray crystallographic data show the fullerene molecule located in the center of a doubly concave cleft with most of the corannulene pincer carbon atoms in van der Waals contact with the fullerene cage with the shortest distance of 3.128 Å. An NMR titration experiment gave an association ($K_a$) constant value of $8600 \pm 500\,M^{-1}$.

A more recent variable-temperature scanning tunneling microscopy (STM) study has provided further evidence for significant π–π interactions between corannulene and $C_{60}$ by imaging corannulene-$C_{60}$ complexes on a Cu(110) surface.[20] Xiao et al. first vapor-deposited corannulene onto the Cu(110) surface and then vapor deposited the fullerene $C_{60.}$ Topographic STM images revealed corannulene-$C_{60}$ complexes, and attempts to relocate the $C_{60}$ away from the corannulene using the STM tip indicated a strongly bound corannulene-$C_{60}$ complex.

### 1-2-2. Theoretical Models of π–π Interactions

The complexity of the synthesis of molecular tweezers and clips mandates the utilization of computational models to design and identify synthetic targets with the desired π–π interactions. Unfortunately, the large size of these molecules and their complexes currently precludes using methods such as CCSD(T) or QCISD(T) that approach chemical accuracy. Therefore, it is critical to understand the limitations and advantages of the lower-level methods, such as molecular mechanics, Hartree–Fock (HF), and density functional theory (DFT), in their application to fullerene receptor design.

Since dispersion interactions arise from electron correlation, low-level computational methods cannot be expected to accurately predict binding energies of weakly bonded molecular complexes. Hartree–Fock molecular orbital (MO) methods (both semiempirical and *ab initio*) do not see dispersion interactions at all and, as a result, underestimate van der Waals interactions.

Density functional theory (DFT) is cost-effective, and calculations on large molecular systems can be run in a reasonable time. It has long been known that although *exact* DFT would include all correlation effects (dispersion interactions), the most popular functionals do not.[21] Until 2006, commonly used density functional methods still did not include long-range interactions, which are the basis of dispersion forces.[22] Since 2000 there has been a surge in research aimed at including dispersion interactions in DFT in order to couple the cost efficiency of DFT with the increased chemical accuracy achieved by accounting for dispersion interactions.[23] Numerous methods are now available that allow DFT to account for dispersion interactions.[24] Faced with these competing methods and new ones being added yearly, researchers encounter the dilemma of which method to employ and how accurate it will be. This can be resolved only by understanding each method's range of application and limitations.

We will discuss two methods commonly used to include dispersion interactions. While there may be better methods available, we have experience using these methods and have found them reliable after comparing our theoretical results to our experimental data.

One method of including dispersion interactions in DFT adds an empirically derived dispersion term to the DFT total energy and is known as DFT-D.[25] We have used one of these DFT-D methods, B97-D developed by Grimme,[25a] in our research. The details of our calculations are discussed later. The B97-D method has proved to be in close agreement with the CCSD(T) potential energy curves of several weakly bound dimer systems, including the benzene dimer.[26]

The second avenue, taken by Truhlar and others, is to reparameterize a functional to include dispersion interactions.[27] Truhlar's latest suite of functionals, M06 class, supercede his earlier M05 class. The M06-2X, M05-2X, M06-HF, M06, and M06-L are all recommended for the study of noncovalent interactions. One test compared the binding energy curves for the benzene–methane dimer calculated using 12 density functionals [each with the 6-311+G(2df,2p) basis set] to both MP2/CBS and CCSD (T)/CBS results. The M05-2X, M06-2X, and M06-HF functionals compared well with the CCSD(T)-calculated binding curve.[27a]

A few years ago there were no options for calculating the noncovalent interactions between large molecules. Now there are several, and more are added yearly. It can be confusing and as Truhlar points out, some have started to question the need for the frequent debut of new functionals.[27b] The reality is that while these methods are improving, none give chemically accurate results. The good news is that, until computer power and the computational codes are able to handle large molecules with the highest level of theory, we now have viable and reasonably accurate methods to calculate noncovalent interactions.

Considering the computational limitations, it is not surprising that the influence of buckybowl curvature on buckybowl π–π stacking interactions has not been exhaustively studied by theoretical methods. After all, the model system, the corannulene dimer, possesses 40 carbon atoms and 20 hydrogen atoms, a significant size increase as compared to the benzene dimer. The early study by Tsuzuki considered the convex–convex corannulene dimer as a model for the convex–convex interaction of two $C_{60}$ cages (Figure 1-4). At the MP2/6-311G(2d) level, the binding energy was calculated as 13.4 kcal/mol with the minimum-energy separation of the central five-membered rings of 3.2 Å.[28] More recently, the binding energy obtained with the

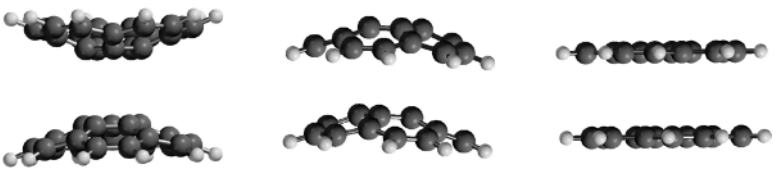


**Figure 1-4.** Conformations of the π–π stacked corannulene dimers.

reparameterized B97-D method of 6.2 kcal/mol at the separation distance of 3.55 Å was mentioned by Peverati and Baldridge without any further discussion of the result.[29] A more detailed study of the stacking interactions of the convex–concave dimer and its "planarized" version (Figure 1-4) was reported by Sygula and Saebo.[30] The best estimate of the binding was 17–18 kcal/mol with the equilibrium distance of 3.64 Å at the SCS-MP2 level of theory with augmented cc-pVTZ basis set. This study also demonstrated that the π–π stacking of curved surfaces is of comparable magnitude as for planar systems of the same size, since the best estimation of the binding in the "planar" dimer (i.e., the dimer in which both corannulene subunits were forced to adopt planar conformations) was 18–20 kcal/mol. However, it has to be pointed out that ~15% of the binding energy in the concave–convex dimer can be attributed to the electrostatic dipole–dipole attraction, which is absent in the "planar" dimer.

Since the dispersion-corrected DFT functionals became available, more computational studies have been reported for even larger systems, including geometry optimization and binding energy calculations for the $C_{60}$@buckycatcher supramolecular complex. These results will be discussed in greater detail later.

While computation[al chemistry can predict properties, eventually the molecule must be synthesized. We start with the half-century pursuit of a simple bowl.

## 1-3. SYNTHESIS OF BUCKYBOWLS

### 1-3-1. Corannulene: From Solution to the Gas Phase and Back

The presence of a pentagonal hub in corannulene induces its bowl shape but also introduces extra strain as compared to planar benzenoid compounds. It is therefore not surprising that the standard synthetic procedures leading to the formation of additional benzene rings in planar PAHs are not successful when applied to the synthesis of buckybowls from the strainless precursors. The original synthesis of corannulene was achieved by a 17-step synthesis starting from acenaphthene with an overall yield of 0.4% (Scheme 1-1).[8] The remaining three six-membered rings were built one at a time around the core five-membered ring to produce a highly hydrogenated intermediate **4,** which was subsequently reduced to corannulene (**2**). Apparently, the main motif of the synthesis was to build up the strain stepwise and as late as possible.

The novelty of **2** attracted considerable attention following the Barth–Lawton communication, but the chemistry and properties of corannulene were not studied

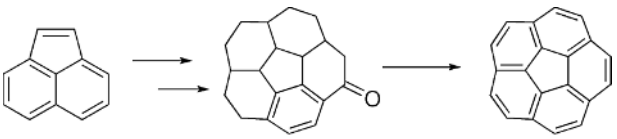


4 2

**Scheme 1-1.** Barth–Lawton synthesis of corannulene.

thoroughly because of the very limited supply of this compound. The original synthetic route was simply too lengthy and laborious. A better synthetic route had to be found.

It was recognized early that fluoranthene (**5**) derivatives represent very attractive synthetic precursors to corannulenes, since they possess four of the six rings of **2** already placed in the right locations. Unfortunately, several Friedel–Crafts cyclization attempts using fluoranthene-7,10-diacetic acid (**6**) or the corresponding acid chloride failed to produce any of the expected corannulene derivatives.[31]

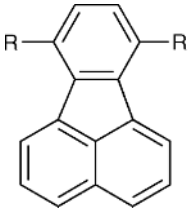


**5:** R = H

**6:** R = COOH, COCl

Obviously, the strain associated with the formation of the corannulene core makes the ring closure processes too slow to be competitive with the intermolecular side reactions leading to oligo- and polymeric products.

A major breakthrough was Scott's 1991 flash vacuum pyrolysis (FVP) methodology for the ring-closing step to produce corannulene from 7,10-diethynylfluoranthene **7** (Scheme 1-2).[32] FVP was performed at high temperatures (~1100°C), providing enough thermal energy to overcome the high activation barriers for the intramolecular ring closures. In addition, the double-cyclization step occurs in the gas phase minimizing unwanted intermolecular side reactions. Subsequently, the FVP-based preparation of corannulene was simplified to only three steps from commercially available starting materials with an overall yield of 26%.[33] In this case the more robust bischlorovinyl (**8**) served as an immediate precursor for corannulene. Other groups have applied FVP methodology for the synthesis of **2** from various precursors, but in most cases no significant improvement in overall yield has been achieved.

Numerous buckybowls have been synthesized by the FVP method,[10b] most notably cyclopentacorannulene (**9**, $C_{22}H_{12}$),[34] the first buckybowl larger than corannulene; two isomeric semibuckminsterfullerenes (**10** and **11**),[35] and circumtriindene (**12**, $C_{36}H_{12}$).[36] Ultimately, formation of buckminsterfullerene $C_{60}$ was achieved by FVP of a $C_{60}H_{27}Cl_3$ polyarene precursor.[37]

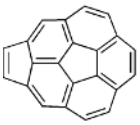

**9**

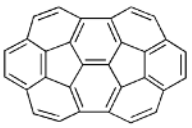

**10**

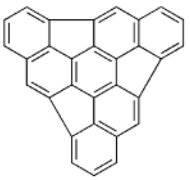

**11**

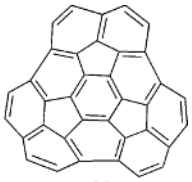

**12**

Despite FVP's undisputable success in preparation of buckybowls, it has several drawbacks. These include technical difficulties with scaling it up; basically no

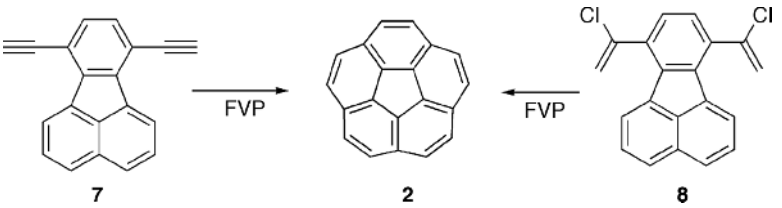


**Scheme 1-2.** Scott's FVP synthesis of corannulene.

functional group tolerance; and dramatically lower yields for larger, less volatile precursors. It soon became clear that practical solution-phase synthetic methodologies needed to be developed to allow for more thorough studies of buckybowls.

In 1996, Siegel reported a solution-phase synthesis of 2,5-dimethylcorannulene (**13**) from tetrabromide (**14**) by low-valence titanium coupling followed by DDQ dehydrogenation with a combined 18% yield for the two steps.[38] Siegel's approach represented just the second successful "wet" synthesis of the corannulene network, 30 years after the original Barth–Lawton work. The success of the formation of the strained corannulene framework was originally attributed to the intermediacy of high-energy organotitanium compounds. Indeed, low-valence titanium and vanadium intramolecular coupling of carbonyl (McMurry coupling)[39] or bromomethyl groups[40] has been known for some time as an effective methodology for the formation of strained ring systems. However, as we will discuss later in greater detail, the major reason for the success of the corannulene formation by Siegel's approach is that the precursor **14** (Scheme 1-3) suffers from severe steric strain caused by the proximity of the bromomethyl and bromoethyl groups in the "bay" regions of the fluoranthene core. The X-ray crystal structures of **14** and its parent hydrocarbon reveal a significant twist of the fluoranthene unit clearly caused by the steric hindrance of the alkyl or bromoalkyl substituents at C1, C6, C7, and C10.[38b]

Following Siegel's success, we tried to apply the same methodology to the synthesis of semibuckminsterfullerene (**10**), which we prepared previously using FVP but in low yield.[35a] Octamethylindenofluoranthene (**15**) was synthesized, and its X-ray crystal structure confirmed its highly nonplanar nature, indicating the presence of significant steric strain caused by the methyl groups located on the rim of the aromatic network.[41] However, numerous attempts using low-valence titanium or vanadium treatment of the octabromide **16** failed to produce any detectable amounts of the expected intramolecular coupling product (Scheme 1-4). In contrast, a respectable 20% yield of **10** was

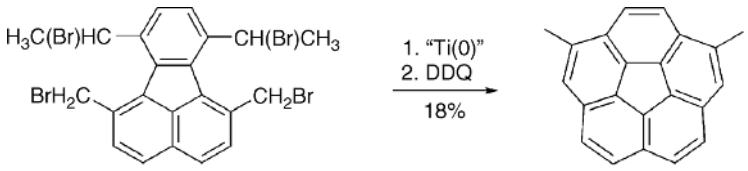


**Scheme 1-3.** Siegel's "wet" synthesis of 2,5-dimethylcorannulene.

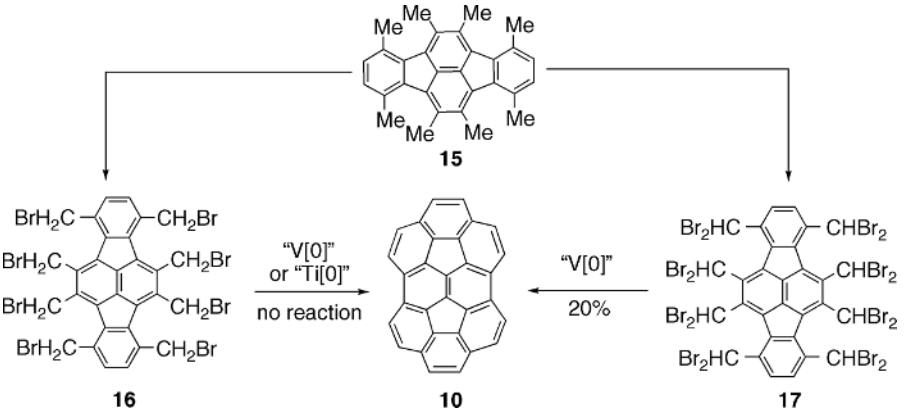


**Scheme 1-4.** Nonpyrolitic synthesis of semibuckminsterfullerene **10**.

achieved by low-valence vanadium treatment of dodecabromide (**17**). We were delighted to find that in contrast to the coupling of bromomethyl groups in **14**, which leads to the formation of a tetrahydrocorannulene core, the coupling of bromomethyl with dibromomethylene groups produces the aromatized product **10** presumably by HBr elimination following the initial ring forming coupling.[41]

The synthesis described above achieved the first solution-phase preparation of a buckybowl larger than corannulene. In addition, it raised the question of whether dibromomethyl groups are more effective precursors than bromomethyl analogs for the coupling leading to formation of the strained ring systems. This was tested by us and independently, by Siegel, on octabromide (**18**), which, on treatment with low-valence vanadium[42] or titanium[43] under high-dilution conditions, produces corannulene in an impressive 70–80% yield (Scheme 1-5).

In an attempt to produce corannulene tetraaldehyde by basic hydrolysis of the dibromomethyl groups in **18**, we serendipitously discovered a novel, low-cost procedure for formation of the corannulene core.[44] The classic hydrolysis method of refluxing **18** in aqueous acetone with $Na_2CO_3$ failed to produce any detectable amount of the expected aldehyde but instead resulted in a carbenoid double ring closure leading to a mixture of brominated corannulenes $C_{20}H_{10-n}Br_n$ ($n = 1-4$) in high yield! This mixture can subsequently be debrominated to produce corannulene in 50–55% yield for the two steps combined. Optimization of the reaction conditions resulted in a simple procedure consisting of a brief 15-min reflux of **18** in aqueous

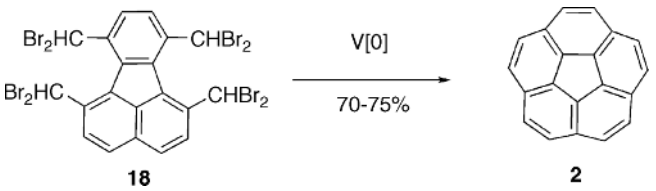


**Scheme 1-5.** High-yielding low-valence vanadium coupling of dibromomethyl groups.

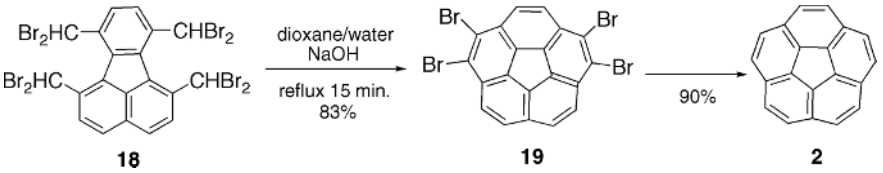


**Scheme 1-6.** Synthesis of the corannulene core by carbenoid coupling of octabromide (**18**).

dioxane with NaOH that produced 1,2,5,6-tetrabromocorannulene (**19**) in 83% isolated yield (Scheme 1-6).

This procedure has several advantages compared to the previous low-valence titanium/vanadium method, including cost, time, and simplicity of the preparation. The previous preparations required high-dilution applications (i.e., a slow, usually overnight addition of the solution of **18** by a syringe pump) and strict anhydrous/oxygen-free conditions (inert-gas atmosphere, dry degassed DME or THF solvents). In contrast, the present preparation can be successfully performed by a first-year undergraduate student assembling a round-bottomed flask with a reflux condenser. The reaction is completed in 15 min, and the separation of the product is trivial since **19** is quite insoluble in common organic solvents, so it is simply filtered from the reaction mixture, washed with water, and dried. The resulting 1,2,5,6-tetrabromocorannulene can be reduced to corannulene in high yield by palladium-catalyzed debromination[45] or used as a starting material for the synthesis of the rim-derivatized corannulenes.[46]

We discovered later that the ring closure of polybrominated systems such as **18** to form the corannulene core can be achieved under milder conditions with metal powders. For example, heating of hexabromide (**20**) with commercial nickel powder in DMF produced 1,2-dicarbmethoxycorannulene (**21**) in 60% yield (Scheme 1-7).[47]

The successful high-yield formation of the corannulene core from benzylbromides of 1,6,7,10-tetramethylfluoranthene under relatively mild conditions may look surprising considering the well-documented fruitless attempts to synthesize corannulene by Friedel–Crafts-type chemistry using 7,10-disubstituted fluoranthenes (e.g., **6**) as precursors.[31] The main reason for the success of the former approach is that a significant amount of strain is built into the precursors (1,6,7,10-tetrasubstituted fluoranthenes), which renders the final intramolecular ring closure favorable, due to the release of the strain. Crystal structure determination proves that both the hydrocarbons (e.g., tetramethylfluoranthene and **15**) as well as their

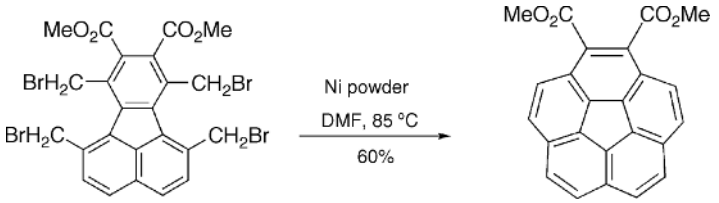


**Scheme 1-7.** Nickel-powder-induced formation of the corannulene core.

brominated derivatives suffer severe steric hindrance of their rim methyl, bromomethyl, and/or dibromomethyl substituents, resulting in a significant twisting of the PAH cores.[38b,48] In contrast, 7,10-disubstituted fluoranthenes can avoid the hindrance by a rotation of the rim substituents away from the hydrogen atoms at C1 and C6. Simple molecular mechanics method 2 (MM2) calculations confirm the explanation that the steric repulsion introduced by the bulky rim substituents raises the energy of the molecule enough to render product formation energetically favorable.[46a]

Availability of corannulene on a gram scale allowed for more systematic studies of its chemistry and for preparation of several derivatives using **2** as a starting material. More recent review articles summarize the progress in the field.[10a,c] Now we will detail the synthetic methodologies for construction of large molecular architectures embedding corannulene units with a potential for the formation of the supramolecular assemblies with various guest molecules, including fullerenes.

### 1-3-2. Corannulene-Based Synthons: 1,2-Didehydrocorannulene and Isocorannulenofuran

The Diels–Alder cycloaddition reaction is often used to construct large conjugated systems from the proper diene and dienophile pair of building blocks. In our pursuit of a practical synthesis of polycyclic aromatic hydrocarbons possessing corannulene subunits, we focused our attention on the previously unknown 1,2-didehydrocorannulene (**22**, a reactive dienophile), and the complementing diene, isocorannulenofuran (**23**). These building blocks promised an easy access to Diels–Alder adducts with corannulene subunits.

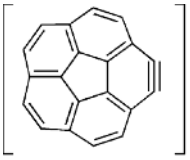

**22**

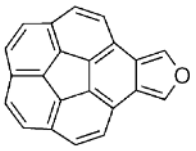

**23**

Originally we attempted the preparation of corannulyne by the well-known anthranilic acid route starting from the available dimethylcorannulenodicarboxylate (**21**). However, despite numerous attempts, we failed to find a useful procedure for the conversion of imide (**24**) to antranilic acid (**25**) [Scheme 1-8(a)]. We therefore turned our attention to alternative methods of benzyne generation and discovered that the *ortho*-deprotonation of easily accessible bromocorannulene (**26**) with sodium amide/potassium tertbutoxide in THF resulted in the formation of corannulyne adducts with the trapping dienes and amines [Scheme 1-8(b)].[49] These adducts were isolated with good yields (70–80%) demonstrating the synthetic usefulness of the approach.

It must be noted that the very harsh conditions required for corannulyne generation by the *ortho*-deprotonation procedure seriously limits the scope of this approach to base-resistant trapping agents. We therefore developed an alternative method for the mild generation of **22** from 2-TMS-corannulennyl triflate (**28**).[50]

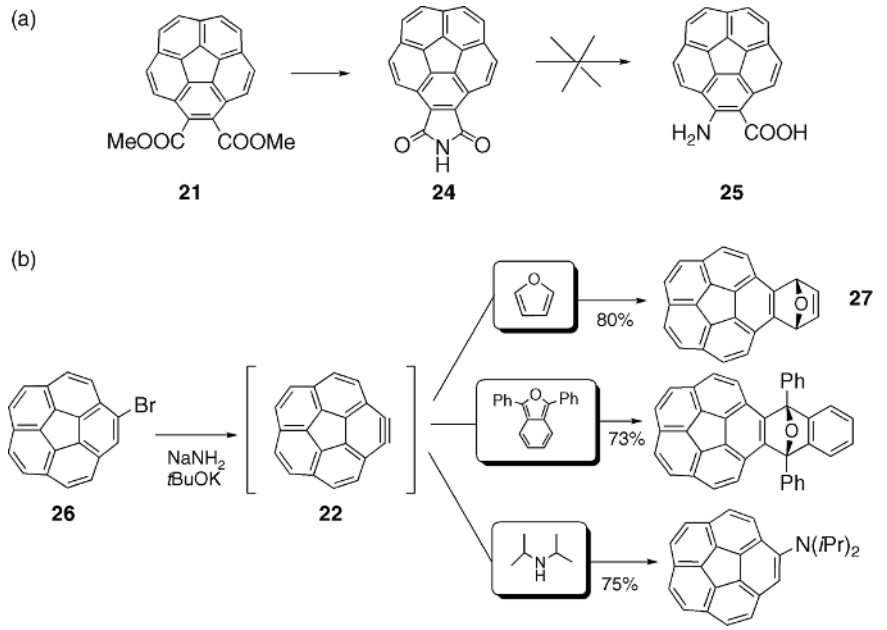


**Scheme 1-8.** (a) Unsuccessful attempts to corannulyne by the anthranilic acid route; (b) generation of corannulyne from bromocorannulene.

*o*-Trimethylsilylaryltriflates have been used as benzyne precursors because the elimination of the TMA and OTf groups can be achieved under very mild conditions by treatment with fluoride anions. Appropriate phenols are typically used as starting materials in the synthesis of these precursors.[51] Unfortunately, hydroxycorannulene was found to be quite unstable and could not be used as a starting material for the synthesis of **28**. We therefore developed an alternative route that started with bromocorannulene (**26)** (Scheme 1-9). Copper-catalyzed etheration of **26** with sodium methoxide led to methoxycorannulene, which was then *ortho*-brominated to produce **29** in good yield. The conversion of **29** to the corresponding *o*-bromophenol

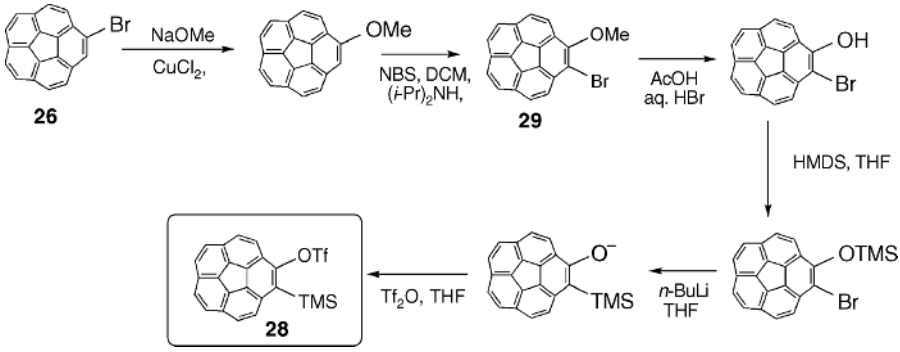


**Scheme 1-9.** Synthesis of *o*-TMS triflate (**28)**.

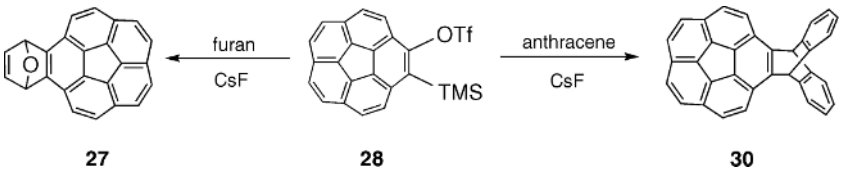


**Scheme 1-10.** Mild generation of corannulyne from **28**.

was achieved by brief reflux in AcOH with aqueous HBr, and the resulting phenol was quickly converted to the *o*-bromotrimethylsilyl ether, which, on metallation with *n*-BuLi at low temperature followed by quenching with triflic anhydride, produced **28** in modest yield of ca. 40% (from **29**). Both *o*-bromophenol and its TMS ether are rather unstable, so they were not purified but quickly converted to the final product **28**. In contrast, *o*-TMS-corannulenyl triflate is stable enough to be stored for weeks with no any evidence of decomposition. Its potential as a precursor for corannulene was tested by trapping experiments with dienes (e.g., furan and anthracene), which produced high yields (78–85%) of the respective adducts. The best results were achieved when the mixture of **26** with the trapping diene in acetonitrile was sonicated at slightly elevated temperatures with two equivalents (2 eq) of CsF.[50]

While trapping corannulyne generated from **28** with furan produces adduct **27** in yields quite similar to that of our original base-induced *o*-deprotonation method, the high-yield formation of anthracene adduct **30**[50] represents an example of the process that we failed to complete by the previous method.[49] This and other examples that we will discuss later prove the versatility of *o*-TMS triflate (**28)** for the synthetically useful generation of 1,2-didehydrocorannulene (Scheme 1-10).

The availability of endoxide (**27)** allows the generation of isocorannulenofuran (**23)** by the well-established *s-tetrazine approach*. Indeed, brief heating of **27** with the commercially available 2,6-bis-2-pyridyl-1,2,4,5-tetrazine provides **23** in an excellent 94% yield (Scheme 1-11).[52]

Isobenzofurans, known for their versatility as reactive dienes in Diels–Alder cycloadditions, are usually too unstable to be isolated, so they are often generated *in situ*. We were pleased to find that **23** is stable enough to be isolated, fully characterized by spectroscopic methods, and stored (as a solid) for several weeks under inert atmosphere with no sign of decomposition. On the other hand, solutions of **23** undergo slow decomposition when exposed to air and/or light, indicating its reactivity. The versatility of **23** in Diels–Alder cycloaddition reactions with benzynes was proved by the formation of endoxides **31–33** with good yields (Scheme 1-11). Deoxygenation of these and related endoxides provides a synthetically useful route to large PAHs with embedded corannulene subunits.[52]

In summary, the synthetic strategy for preparation of large PAHs with corannulene subunits developed in our laboratory is based on employment of three methods:

*Method A*. Introduction of 1,6,7,10-tetramethylfluoranthene unit to the appropriate molecular scaffold followed by a radical (di)bromination of the dangling methyl groups and a subsequent ring closure induced either by treatment with NaOH in aqueous dioxane or by nickel powder in DMF to generate the corannulene core.

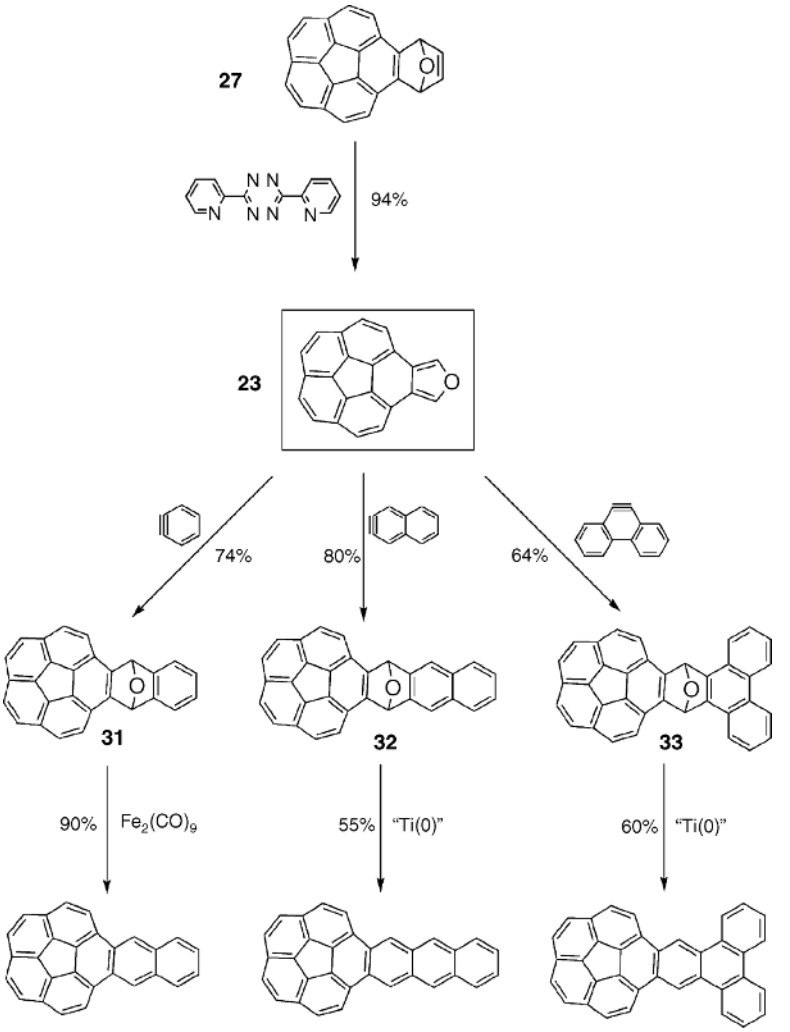


**Scheme 1-11.** Synthesis and Diels–Alder cycloaddition reactions of isocorannulenofuran (**23**).

*Method B*. Introduction of the corannulene subunit by Diels–Alder cycloaddition reaction of corannulyne (**22**) [generated from either bromocorannulene (**26**) or from *o*-TMS triflate (**28**)] with an appropriate diene.

*Method C*. Introduction of the corannulene subunit by Diels–Alder cycloaddition reaction of isocorannulenefuran (**23**) with an appropriate dienophile.

The following section describes our successes as well as failures encountered when applying this strategy to construct highly nonplanar molecular constructs with corannulene subunits that have the potential to act as molecular receptors for guest molecules with a special focus on fullerene cages.

## 1-4. TOWARD MOLECULAR CLIPS AND TWEEZERS WITH CORANNULENE PINCERS

### 1-4-1. Twin Corannulene: The First Attempt

The lack of experimental evidence for the formation of concave–convex stacked supramolecular assemblies of corannulenes with fullerenes in solution indicates that the attractive dispersion interaction of a single corannulene bowl with the convex surface of a fullerene cage is insufficient to overcome the expected entropy and solvation penalties associated with the dimeric complex formation. We therefore turned our attention to the design and synthesis of more complex molecular architectures with at least two corannulene pincers attached to a tether in a pre-organized way to form a cavity large enough to accommodate $C_{60}$ as a host molecule.

Our first attempt led to the synthesis of "twin corannulene" (**34**), namely, dicorannulenobarrelene dicarboxylate.[53] The synthesis started with cyclopentadienone (**35**) (an intermediate in the corannulene synthesis), which undergoes a double Diels–Alder cycloaddition to 1,2-benzoquinone (Scheme 1-12). This one-pot process afforded target anthraquinone (**36**) in good yield. Quinone (**36**) was subsequently reduced to anthracene (**37**) by aluminum cyclohexide in cyclohexanol. Diels–Alder

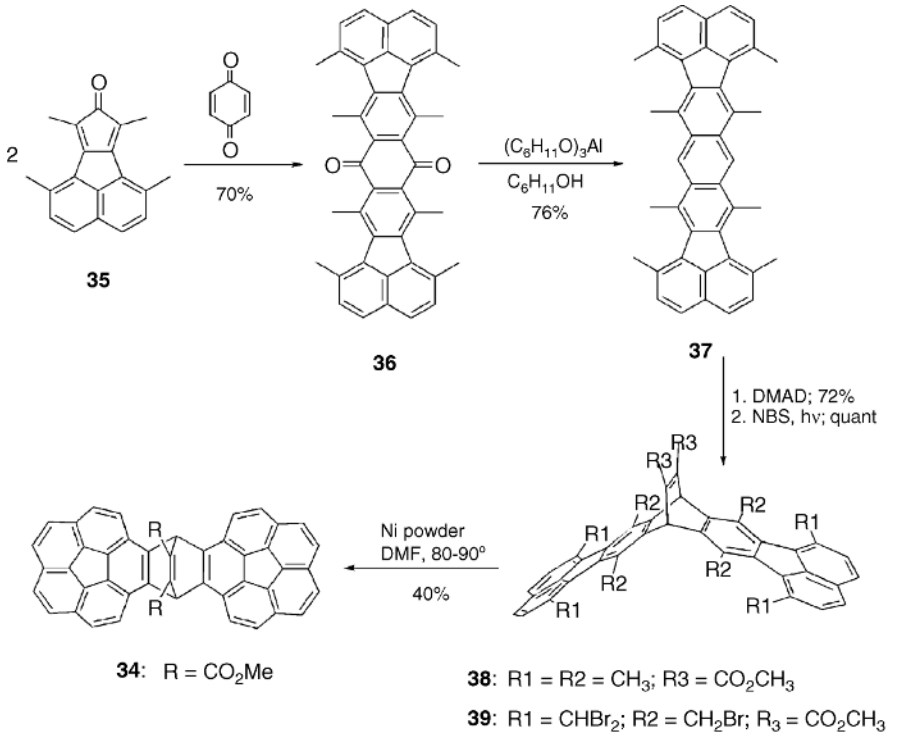


**Scheme 1-12.** Synthesis of "twin corannulene" (**34**).

cycloadditon of dimethylacetylenedicarboxylate to **37** provided difluoranthene barrelene (**38**), which was subsequently brominated under forcing conditions to produce dodecabromo derivative **39**. The bromide underwent fourfold ring closure on treatment with nickel powder to form dicorannulenebarrelene (**34**) in a respectable 40% yield.[53]

Twin corannulene (**34**) represents the first example of a potential molecular clip with two corannulene pincers and a barrelene tether. Three possible conformers of **34** should exist because of the inversion of the corannulene bowls. While the room temperature (rt) $^1$H NMR spectrum of **34** is quite simple, exhibiting only five different proton signals due to the time-averaged $C_{2v}$ symmetry of the molecule, at low temperatures the presence of three different species with approximate populations of 0.82, 0.13, and 0.05 is revealed by the splitting of the carbomethoxymethyl protons (a singlet at 3.80 ppm at rt) into three signals at 4.01, 3.71, and 3.40 ppm at −78°C (Figure 1-5). In

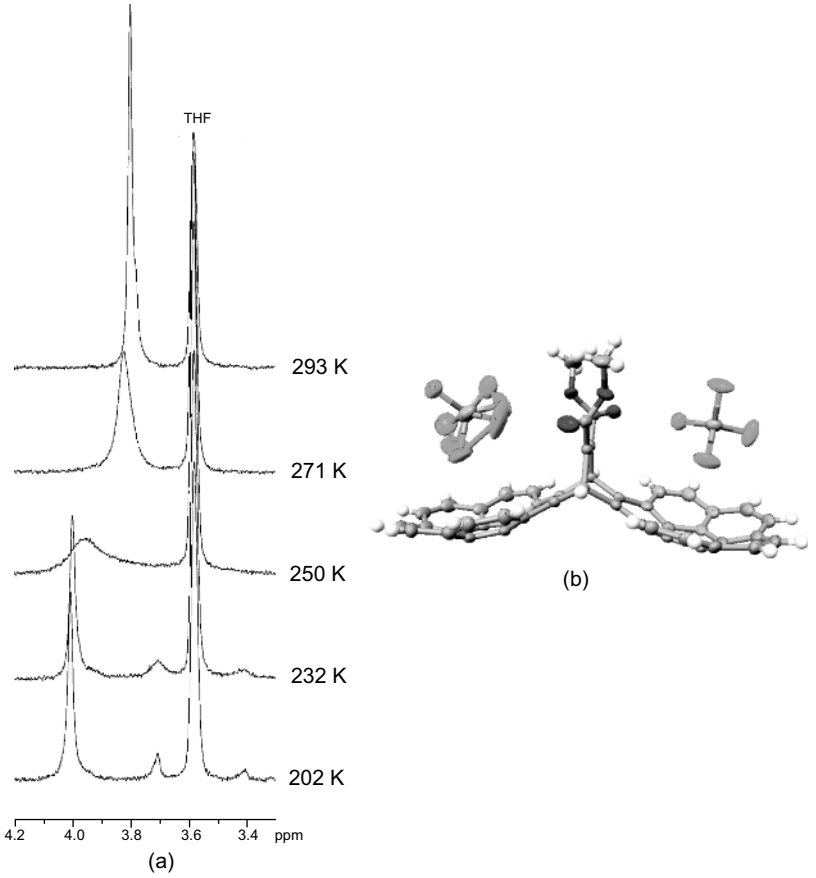


**Figure 1-5.** (a) Variable-temperature $^1$H NMR spectra of the carbmethoxymethyl protons of **34** in THF-$d_8$; (b) X-ray crystal structure of **34** with two $CCl_4$ solvating molecules (one $CCl_4$ molecule is disordered).

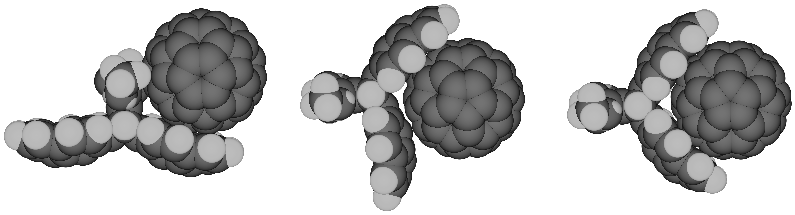


**Figure 1-6.** MM2 geometries and relative stabilities of $C_{60}$@**34** assemblies.

line with the experiment, B3LYP/6-311G**//B3LYP/3-21G calculations reveal that all three conformers of **34** have quite similar energies with the *exo–exo* conformer (**34a**) predicted to be most stable and the *endo–endo* conformer (**34c)** to be least stable. X-ray analysis shows that **34a** is also preferred in the solid state. Compound **34** incorporates two $CCl_4$ molecules into the crystal lattice, occupying the concave surfaces of the corannulene pincers (Figure 1-5).[53]

The presence of a significant cavity formed by the corannulene pincers permits the intriguing possibility that **34** might act as a host molecule in supramolecular assemblies. The *endo–endo* variant (**34c)** appears to be the best candidate to host a fullerene cage inside the cavity defined by the two concave surfaces of the pincers. Its slightly higher energy, as compared to the other two conformers of **34**, does not eliminate **34c** from the competition since MM2 calculations predict the $C_{60}$@**34c** complex to be more stable than the analogous complexes of $C_{60}$ with either **34a** or **34b** by ~4 kcal/mol (Figure 1-6). Obviously, the *endo–endo* conformation of **34** allows for more efficient π–π stacking of both concave surfaces of the pincers with the convex surface of $C_{60}$. Because of the relatively low inversion barrier of corannulenes, equilibration of various conformers of **34** is quickly achieved at ambient temperatures. In addition, our MM2 calculations estimate a significant binding energy for the $C_{60}$@**34** complex formation (19.5 kcal/mol). Taking these results into account, we concluded that **34** would be a legitimate candidate for a molecular clip capable of hosting $C_{60}$ in a supramolecular assembly.

Unfortunately, we were not able to detect the complexation of $C_{60}$ by **34** experimentally. Several attempts to cocrystallize the two compounds from various solvents failed to produce any mixed crystals. Also, nuclear magnetic resonance (NMR) experiments did not show any significant changes in the chemical shift of the protons of **34** on titration with $C_{60}$ solutions.

### 1-4-2. A Buckycatcher Enters the Game

Searching for alternative tethers to incorporate into biscorannulene molecular clips, we turned our attention to dibenzocyclooctadiyne (**40**), which is an attractive candidate for the synthesis of highly nonplanar molecular networks. Although this

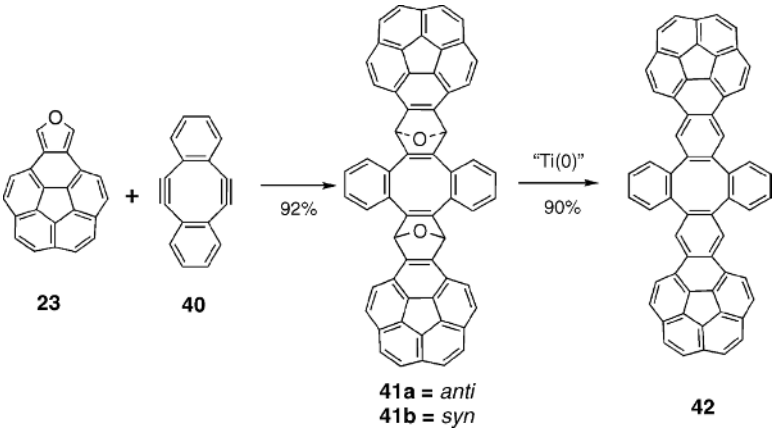


**Scheme 1-13.** Synthesis of buckycatcher $C_{60}H_{28}$.

dienophile is quite reactive toward dienes, it is stable enough to be stored for several weeks. Preparation of **40** is quite straightforward and, in addition, a double-Diels–Alder cycloaddition of an appropriate diene will generate the tetrabenzocyclooctatetraene scaffold, which exhibits some steric flexibility but, at the same time, has a significant inversion barrier keeping the newly generated pincers on the same side of the core.[54] We used isocorannulenofuran **23** as the diene that contributes corannulene subunits to the Diels–Alder adducts.[19] Thus, 2 eq of **23** reacted with dibenzocyclooctadiyne (**40)** to produce a mixture of two isomeric adducts, **41a** and **41b,** with a combined yield of 92% (Scheme 1-13). As judged by their NMR spectra, the major adduct exhibits $C_s$ symmetry, while the minor product has $C_{2v}$ symmetry. The X-ray crystal structure of **41a** confirmed that the major product resulted from the *anti*-bis addition of **23** to diyne (**40)** (Figure 1-7).

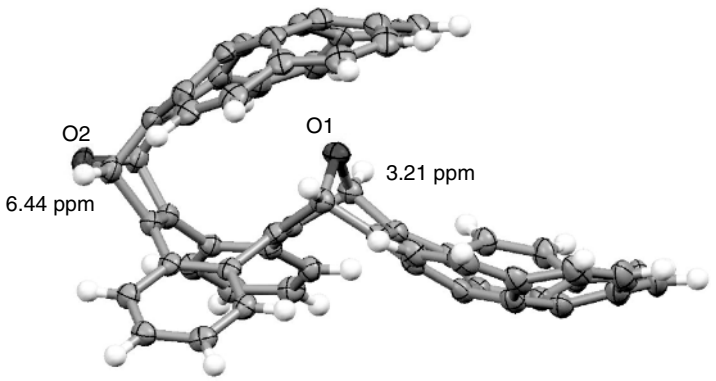


**Figure 1-7.** Crystal structure of the major adduct **41a**. A solvating toluene molecule is omitted for clarity. $^1$H NMR chemical shifts of the bridgehead hydrogen atoms "inside" and "outside" the upper corannulene unit are shown.

Adduct **41a** exhibits a high degree of nonplanarity; as a result of the anti addition, one of the bridging oxygen atoms (denoted O1 in Figure 1-7) as well as the two bridgehead hydrogen atoms connected to the O1-neighboring carbon atoms are located "under the umbrella" of one of the neighboring corannulene subunits. These protons are strongly magnetically shielded by the corannulene fragment, resulting in an upfield shift (3.21 ppm), while the resonance of the other two bridgehead protons (close to O2) is observed at 6.44 ppm.[19]

The minor adduct **41b** has not been characterized by X-ray crystallography; however, on the basis of its NMR spectra, which indicate $C_{2v}$ symmetry and the typical chemical shifts of the four symmetry equivalent bridgehead hydrogen atoms (6.33 ppm), we conclude that it results from *syn* bis addition of **23** to diyne (**40**).

Deoxygenation of both isomers of **41** was achieved by the low-valent titanium method to produce the target hydrocarbon $C_{60}H_{28}$ (**42**).[19] In analogy to the case of dicorannulenobarrelene (**34**), we anticipated three possible conformations of **42a–42c**, quickly interconverting through bowl-to-bowl inversions of the corannulene subunits. Quite recently we realized that the tether's flexibility makes possible an unrecognized conformer (**42d**), exhibiting internal π–π stacking of the corannulene pincers.[55] Our recent computational study demonstrates that the π–π binding energy of the concave–convex corannulene dimer is quite substantial,[30] which could compensate for a significant bending penalty in the deformed TBCOT tether in **42d**. At the MM2 level of theory, **42d** represents a global minimum, more stable by ~2 kcal/mol than the "open" conformers **42a–42c**. The geometries of the four conformers of **42** along with their relative energies calculated at B97-D/TZVP and B97-D/cc-pVQZ levels of theory are shown in Figure 1-8.[55]

The TZVP and cc-pVQZ basis sets are large enough to minimize the basis set superposition error (BSSE), a very important factor for the accurate calculation of binding energies of π–π stacked systems. As shown previously by Grimme, BSSE accounts for approximately 10% of the dispersion interaction energy at B97-D/TZVP.[56] We have demonstrated that BSSE is almost completely eliminated when the very large cc-pVQZ basis set is used (thus reaching the *complete basis set* limit), so the numbers shown in Figure 1-8 represent the accuracy limit of the B97-D functional.

| | 42a | 42b | 42c | 42d |
|---|---|---|---|---|
| TZVP | 0.55 | 0.72 | 0.97 | 0.00 |
| cc-pVQZ | 0.13 | 0.34 | 0.47 | 0.00 |

**Figure 1-8.** B97-D calculated structures and relative energies (kcal/mol) of the conformers of buckycatcher **42**.

The stabilities of all four conformations of **42** lie within 0.5 kcal/mol of each other at the highest level of theory applied. Considering the accuracy limitations of the computational theory, it is difficult to declare with certainty which of the isomers is the most stable in the gas phase. However, well-defined but thermally accessible energy barriers separating the conformers bring interesting possibilities of a conformational diversity of **42** in condensed phases since in the presence of a proper complexing solvent or a cosolute, the open conformations may prevail, while in the gas phase or in poorly solvating media, the π−π stacked **42d** could be favored. Generally, solvation effects will favor the open conformations because of their larger solvent-accesible surfaces as compared to **42d**.

The "closed" **42d** represents an unprecedented conformational motif of the terabenzocyclooctatetraene system induced by an intramolecular π−π stacking of the corannulene pincers.[55] Thus, **42d** and the open *exo*−*endo* **42b** equilibrate through a transition state **42TS** (Figure 1-9). At the B97-D/cc-pVQZ level, **42TS** is higher in energy by 4.5 or 4.2 kcal/mol than **42d** or **42b**, respectively. In order to better understand the origins of the unusual "double-dip" bending potential of **42b**−**42d,** we further analyzed the contributions of the attractive π−π stacking of the corannulene pincers and the deformation penalties of the dibenzocyclooctatetraene tether to the total potential energy.[55] The strong π−π stacking of the corannulene pincers in the "closed" conformation **42d** overcomes the energy penalty caused by a significant distortion of the tether. On the other hand, in the open **42b** conformation the relaxation of the tether overcomes the loss of van der Waals attraction of the pincers and the total potential energy reaches another minimum. The origin of a transition state in the "opening" of the tether when going from **42d** to **42b** can then be explained by the loss of the dispersion attraction of the corannulene pincers, which is faster than the relaxation of the TBCOT fragment.

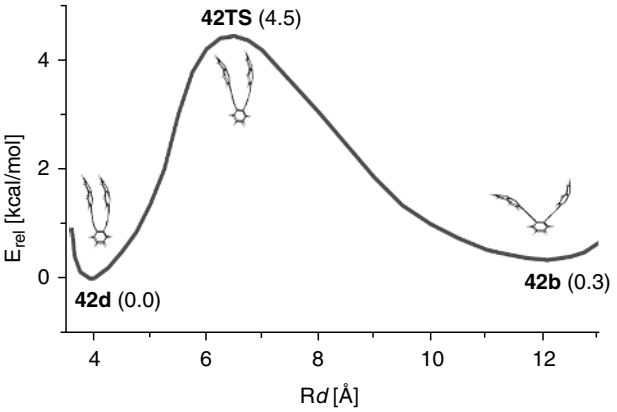


**Figure 1-9.** B97-D/cc-pVQZ "double-dip" bending potential of the *exo*−*endo* conformations of **42**. $R_d$ is the distance between the two most separated carbon atoms of the central five-membered rings of both corannulene subunits. Relative energies (kcal/mol) of the critical points are shown in parentheses.

### 1-4-3. Buckycatcher Complexes with $C_{60}$ and $C_{70}$: A Good Catch

Three of the four conformations of **42** exhibit large cavities defined by the corannulene pincers. *Endo–endo* **42a** appears to be the best candidate to accommodate a molecule of buckminsterfullerene with the two concave surfaces of the pincers available for π–π stacking with the convex surface of $C_{60}$. The distances between symmetry-related carbon atoms in the hub five-membered rings of the two corannulene subunits of the geometry optimized **42a** range from 9.8 to 11.9 Å.[19,55] Since the effective van der Waals radius of $C_{60}$ in its pristine state and in several of its inclusion complexes falls in the range of 9.8–10.2 Å,[57] it is evident that **42a**'s cavity size is compatible with the size of buckminsterfullerene. MM2 calculations predict a binding energy of 24.1 kcal/mol for $C_{60}$@**42a**, significantly higher than the 19.5 kcal/mol calculated for the previously synthesized dicorannulenobarrelene clip **34**. These findings indicated that **42a** should be able to form stable inclusion complexes with fullerenes, in contrast to **34**.

Slow evaporation of an approximately 1 : 1 solution of **42** and $C_{60}$ in toluene produces dark-red crystals.[19] The X-ray crystal structure reveales these crystals to be the inclusion complex $C_{60}$@**42a** with two solvating toluene molecules. There is some disorder in the crystal, which involves the solvating toluene and $C_{60}$. The $C_{60}$ molecule lies on a crystallographic mirror plane, but its molecular mirror plane is rotated out of the crystallographic mirror by approximately 15° about a vector joining opposite six-membered ring centroids. Thus, its 60 carbon sites were assigned half-population. Also, the toluene molecule was modeled with two orientations having populations of 0.54 and 0.46. Buckycatcher **42** also lies on the crystallographic mirror plane that relates the corannulene subunits. Both **42** and the solvating toluene molecules wrap around the "equatorial" region of buckminsterfullerene and allow for the columnar arrangement of $C_{60}$ cages along the crystallographic *a* axis with close contacts of the cages in their "polar" regions [Figure 1-10(a)].[19] The buckminster-

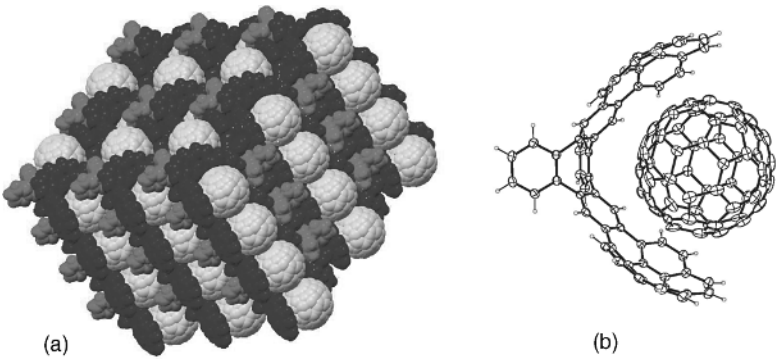


**Figure 1-10.** (a) Crystal packing pattern of **42** (blue) with $C_{60}$ (gold) and toluene (red). Both disordered orientations of $C_{60}$ and toluene are shown. (b) Ortep representation of the arrangement between **42** and $C_{60}$ in the crystal. Only one of the two disordered orientations of $C_{60}$ is shown.

fullerene separation in the crystal defined by the centroid-to-centroid distance of 9.7730(15) Å is at the lower end of the usual 9.80–10.2 Å range observed for other inclusion complexes of $C_{60}$.

The fullerene molecule is placed in the center of a doubly concave cavity formed by the corannulene pincers of **42a** [Figure 1-10(b)]. Examination of the nonbonding carbon–carbon distances between the corannulene pincers and $C_{60}$ indicates close contacts of the two (with the shortest distance of 3.128 Å), confirming that **42,** indeed, acts as a molecular receptor for $C_{60}$. Any detailed discussion of the host–guest interactions in $C_{60}$@**42a** based on the carbon–carbon distances from the X-ray crystal structure is complicated by the disorder of $C_{60}$. Therefore, we analyzed the geometry relations in greater detail by considering distances between the centroid of the fullerene cage and the carbon atoms of the corannulene pincers.[55] This approach allows for a better understanding of π–π host–guest interactions and renders the observed disorder of $C_{60}$ in the crystal state unimportant. Table 1.1 presents the fullerene centroid–buckycatcher carbon distances, which are averaged over the highest possible $C_{2v}$ symmetry of the corannulene pincers of **42a**, regardless of the supramolecular complex symmetry. The experimental[19] distances are compared to the distances calculated at B97-D/TZVP[55] and by M06-L/MIDI! [58] levels. Generally, both computational models reproduce the experimental distances quite well. The calculated intramolecular distances are consistently shorter than the experimental data, with an average deviation of 0.08 Å (B97-D/TZVP) or 0.16 Å (M06-L/MIDI!). On average, B97-D/TZVP reproduces the experimental geometry of the complex slightly better than do the M06-L/MIDI! calculations.

Considering the radius of $C_{60}$ in the complex ($3.543 \pm 0.035$ as found in the crystal) and the van der Waals radius of the $sp^2$-hybridized carbon atom (~1.8 Å), essentially all the carbon atoms of both corannulene pincers are in van der Waals contact with the convex surface of $C_{60}$. The shortest carbon–carbon distance between

**TABLE 1-1. $C_{2v}$ Symmetry Averaged Distances (Å) between the Centroid of the Fullerene Cage and the Pincer Carbon Atoms in $C_{60}$@42a**

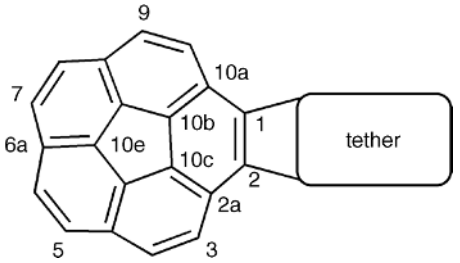


| Method | C1 | C2a | C3 | C4 | C4a | C5 | C6 | C6a | C10b | C10d | C10e | Ref. |
|---|---|---|---|---|---|---|---|---|---|---|---|---|
| X-ray | 6.77 | 6.71 | 6.73 | 6.76 | 6.77 | 6.83 | 6.85 | 6.80 | 6.85 | 6.88 | 6.90 | 19 |
| B97-D | 6.68 | 6.63 | 6.65 | 6.68 | 6.69 | 6.73 | 6.74 | 6.71 | 6.80 | 6.82 | 6.84 | 55 |
| M06-L | 6.54 | 6.51 | 6.58 | 6.63 | 6.62 | 6.72 | 6.74 | 6.67 | 6.65 | 6.69 | 6.72 | 58 |

the host $C_{60}$ and the corannulene pincers in the crystal is 3.13 Å, closely reproduced by both computational models (3.09 Å and 3.10 Å by B-97-D[55] and M06-L,[58] respectively). The distance between the two most widely separated carbon atoms of the central five-membered rings of both corannulene subunits ($R_d$, C10e–C10e′), which describes the size of a cleft in between the corannulene pincers in $C_{60}$@**42** complex, is 12.81 Å in the crystal. This crucial distance is also very well reproduced by both computational methods [12.80 (B97-D) and 12.70 Å (M06-L)].

Nuclear magnetic resonance titration experiments prove that the complexation of **42** with buckminsterfullerene also takes place in toluene solution.[19] Systematic downfield changes in the chemical shifts of the four symmetry-independent protons in the corannulene subunits (i.e., at C3, C4, C5 and C6; see Table 1.1) of **42** are observed on addition of $C_{60}$. The maximum changes in their chemical shifts, defined as $\Delta\delta_{max} = \delta_{bound} - \delta_{free}$, are 0.118, 0.134, 0.102, and 0.099 ppm, while the $\Delta\delta_{max}$ of the remaining three symmetry-independent protons of the TBCOT tether are only −0.06, −0.01, and −0.01 ppm. Assuming the existence of a fast (on the NMR timescale) equilibrium between the supramolecular dimer and the monomeric buckycatcher and $C_{60}$, we can write the following equation:

$$K_a = \frac{[C_{60}@\mathbf{42}]}{[C_{60}] * [\mathbf{42}]} \qquad \text{and} \qquad \delta_H = x * \delta_{bound} + (1-x) * \delta_{free}$$

where $x$ describes the mole fraction of the buckycatcher bound in the supramolecular assembly, that is, $x = [C_{60}@\mathbf{42}]/[\mathbf{42}]_{total}$. These relations lead to the following equation:

$$\Delta\delta = \frac{L(1+K_a * X+K_a * Y)-(L^2 * (1+K_a * X+K_a * Y)^2-4K_a^2XYL^2)^{1/2}}{2K_aY}$$

Here, $X = [C_{60}]_{total}$, $Y = [\mathbf{42}]_{total}$, and $L = \Delta\delta_{max}$.

Nonlinear curve fitting of the experimental changes of the chemical shifts of the clip protons as a function of $[C_{60}]_{total}$ and $[\mathbf{42}]_{total}$ gives an estimation of $K_a$ and $\Delta\delta_{max}$, which are treated as parameters. Figure 1-11 illustrates the experimentally determined chemical shift changes of one of the buckycatcher protons as a function of the concentration of $C_{60}$ along with the curve-fitting results. The curve fitting provided four independent evaluations of $K_a$ values in the range of 8000–9300 $M^{-1}$ with the averaged value of $K_a = 8600 \pm 500\,M^{-1}$.[19]

As we discussed earlier, unsubstituted corannulene does not show any evidence of complexation with $C_{60}$. The same is true for biscorannulenobarrelene **34**, our first potential molecular tweezers with two corannulene pincers. The high value of the association constants for $C_{60}$@**42** complex formation proves, therefore, that the TBCOT scaffold aligns the corannulene pincers properly for the accomodation of fullerene cages in solutions. Not only do the previously reported complexations of *sym*-pentakis(arylthio)corannulenes with $C_{60}$ in toluene ($K_a$ in the range of 60–450 $M^{-1}$)[17a] and decakis(arylthio)corannulene in carbon disulfide ($K_a = 1400\,M^{-1}$)[17b] have much lower association constants; the majority of the binding can be attributed to the rim substituents interacting with $C_{60}$ in these systems. In the case of

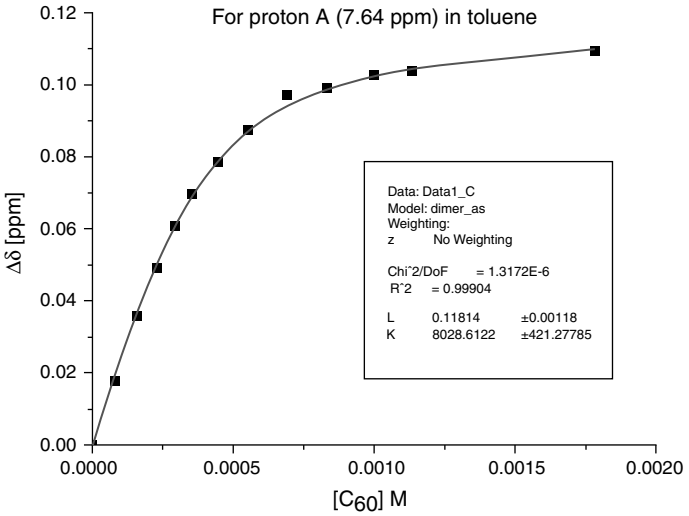


**Figure 1-11.** Chemical shift changes of one of the pincer hydrogen atoms in **42** on $C_{60}$ titration with the nonlinear curve-fitting results.

buckycatcher **42**, the strength of the binding comes from pure dispersion interactions of the convex surface of the fullerene cage with the properly oriented concave surfaces of the corannulene pincers, since no heteroatoms or polar substituents contribute to the binding.

Formation of the supramolecular assemblies of the buckycatcher with fullerenes is strongly influenced by the entropy and solvation penalties. These severe penalties have to be overcome by a very significant binding enthalpy of the supramolecule for a favorable free energy ($\Delta G$) of association. As we discussed previously, accurate assessment of the dispersion energies by the commonly used theoretical models is quite challenging, especially for larger systems. Our report describing the characterization of the $C_{60}$@buckycatcher complex inspired some theoretical studies of the system. The first assessment of the binding energy in $C_{60}$@**42** was reported by Wong, who published the results of a comparative study of the performance of nine popular density functionals on the complex.[59] It is not surprising that seven of the nine functionals failed to predict any binding between $C_{60}$ and the buckycatcher. Only two of the tested functionals—MPWB1K and M05-2X—predict some binding for the complex by 10.2 and 20.7 kcal/mol, respectively. Later, Zhao and Truhlar calculated the binding energy in $C_{60}$@**42** as 26.4 kcal/mol at the M06-2X/DIDZ//M06-L/MIDI! level.[58] Our more recent B94-D/TZVP calculations gave a dramatically higher estimate for the binding energy at ~43 kcal/mol.[55] It has to be pointed out that both M05-2X and M06-2X calculated binding energies were BSSE-corrected, and the corrections were quite substantial, due to the relatively low-quality basis sets employed. In contrast, B97-D/TZVP binding energies were not corrected for BSSE since the error is expected to be lower than 10% of the binding energies at this level of calculation (for a more detailed discussion, see Ref. 56).

The experimental $\Delta G_{293}$ of association of $C_{60}$@**42** in toluene is −5.3 kcal/mol, as calculated from $K_a = 8600\ M^{-1}$, determined by NMR titration experiment.[19] Because of the expected influence of the entropy and solvation on the equilibrium, it is not possible to assess the quality of the computed gas-phase binding energies using the experimentally determined $\Delta G$ value in solution. Zhao and Truhlar estimated the gas-phase free energies of $C_{60}$@**42** formation by the harmonic oscillator–rigid rotator approximation as approximately −7 kcal/mol, while their BSSE-corrected M06-2X/DIDZ//M06-L/MIDI! gas-phase energy of association was −26.4 kcal/mol.[58] The dramatic difference emphasizes the magnitude of the entropy penalty for the supramolecular $C_{60}$@**42** formation. In addition, the association of buckycatcher with $C_{60}$ in solution results in a considerable loss of the solvent-accessible surfaces on both host and guest molecules. Employment of a simple solvation model predicts solvent-accesible surfaces of 429, 776, and 973 Å$^2$ for $C_{60}$, buckycatcher, and $C_{60}$@**42** complex, respectively.[58] Clearly, considerable solvent accesible surface is lost in formation of the supramolecular assembly, which further decreases the exergonicity of the association. The combination of the entropy and solvation penalties imposes a requirement for quite high binding energies of the supramolecular assemblies to enable the hosts to act as molecular receptors for the fullerene cages.

On the basis of previously reported studies of similar and even larger systems, we believe that the binding energy of $C_{60}$@**42** calculated using the B97-D functional represents a more accurate estimate than do the previously reported M05-2X or M06-2X results. The M05-2X functional underestimates the binding in the benzene dimer and, while M06-2X performs better, it still significantly underestimates the dispersion energies at intermolecular distances greater than the equilibrium distance.[60] Since several noncovalent carbon–carbon distances in $C_{60}$@**42** are longer than the sum of the van der Waals atomic radii, it is understandable that M06-2X (or other asymptotically incorrect functionals) predict smaller binding energies than do DFT-D methods.

Two related systems exhibiting π–π stacking of bowl-shaped conjugated carbon networks have been studied: the corannulene dimer (**43**)[29,30] and the $C_{60}$@corannulene complex (**44**).[20] The *exo–endo*-corannulene dimer may be considered as a model system for larger systems exhibiting the convex–concave stacking of curved conjugated carbon surfaces. At the reliable spin-component scaled second order Moller-Plesset (SCS-MP2) level of theory with aug-cc-pVTZ basis set, the best computational estimate of the binding energy in **43** is ∼17–18 kcal/mol, with the minimum-energy separation of the corannulene monomers of 3.64 Å.[30] B97-D/TZVP calculations gave very similar results (17.0 kcal/mol binding with 3.63 Å separation) confirming the reliability of this computational model.[55]

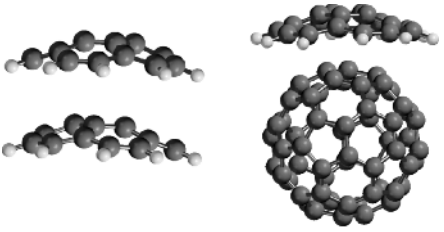

**43** **44**

Calculations using the MP2 method predicted binding energies for the $C_{60}$@corannulene supramolecule (**44**) of 16.1, 17.5, and 24.7 kcal/mol with 6-31G, 6-31G**, and cc-pVDZ basis sets, respectively.[20] The MP2 method is known to seriously overestimate the dispersion forces at the basis set limit, but it was also observed some time ago that with limited basis sets this method can give satisfactory results, due to the cancellation of the two errors, namely, *overestimation* of the attraction by the MP2 approach and its *underestimation* due to the incomplete basis set.[61] We therefore believe that the reported range of 16–24 kcal/mol represents a reasonable estimate of the binding energy in **44**. B97-D/TZVP predicts the binding energy in **44** as 19.5 kcal/mol, in line with the MP2 results. Again, a significantly lower gas-phase binding energy of 12.4 kcal/mol was calculated for **44** at the M06-2X/DIDZ//M06-L/MIDI! level.[58]

Zhao and Truhlar provided a theoretical explanation for the lack of experimental evidence for the supramolecular assembly between $C_{60}$ and corannulene in solution.[58] Calculations of the entropic contributions provided a positive (+5.4 kcal/mol) gas-phase $\Delta G_{293}$ for the formation of **44**. In solution there is an additional solvation penalty caused by the solvent-accesible surface loss on the complex formation, which will surely increase $\Delta G_{293}$ by a few kcal/mol. In contrast to the $C_{60}$@buckycatcher complex, entropy and solvation penalties in $C_{60}$@corannulene override the significant host–guest dispersion attraction, and these results explain why this supramolecular complex has not been experimentally detected in solution.

***$C_{70}$ Complexation by Buckycatcher.*** The ultimate goal in the design and synthesis of molecular clips is to achieve their specificity in binding of guest molecules (molecular recognition). Such specificity may lead to numerous applications of the molecular clips in (among others) separation sciences, catalysis, and material sciences. We tested the potential of buckycatcher **42** for molecular recognition of fullerene cages of diffrent sizes and shapes by a detailed computational study of the energetics of its supramolecular assembly with $C_{70}$ (**45**).[55] We considered three orientations of the oblong $C_{70}$ cage inside the cleft of the buckycatcher (Figure 1-12). Thus, in **45a** the $C_{70}$ axis is aligned within the mirror plane relating the two corannulene bowls of the buckycatcher, but somewhat away from the $C_2$ axis of the clip to better fit the concave shape of the pincers. In **45b**, the $C_{70}$ axis is perpendicular to both the $C_2$ axis and $C_s$ planes of symmetry halving the corannulene pincers. Finally, in **45c** the fullerene axis is perpendicular to the $C_2$ axis but is aligned with the aforementioned plane of symmetry of the clip. B97-D/TZVP gas-phase binding energies and $R_d$ distances, defined as distances between the two most separated carbon atoms of the central five-membered rings of the two corannulene subunits (C10e–C10e′), are presented in Figure 1-12. $C_{60}$@**42** complex data are also included in Figure 1-12 for comparison. The $R_d$ value for the unperturbed *endo–endo* conformer **42a** is 11.15 Å, and any change in this distance within the supramolecular assemblies **45a–45c** describes the degree of buckycatcher deformation caused by inclusion of the fullerene cage. Obviously the corannulene tweezers in **42** have to move apart in order to adopt the guest $C_{70}$ or $C_{60}$. However, as pointed out by Zhao and Truhlar,[58] the buckycatcher is quite flexible for modest changes in its tether geometry,

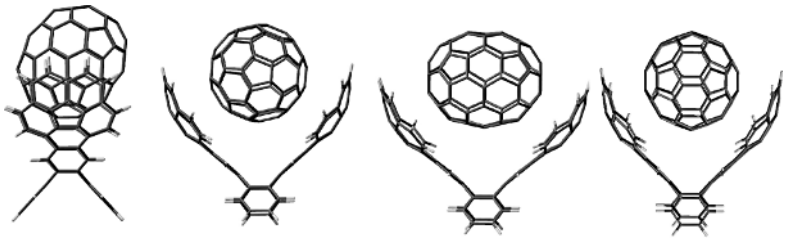

| | **45a** | **45b** | **45c** | $C_{60}$**@42** |
|---|---|---|---|---|
| $E_b$ | 45.1 | 44.0 | 40.3 | 42.8 |
| $R_d$ | 12.78 | 12.94 | 13.50 | 12.80 |

**Figure 1-12.** B97-D/TZVP minimum-energy geometries of three $C_{70}$@**42** and $C_{60}$@**42** compounds with their gas-phase binding energies and $R_d$ values.

so the clip deformation penalties in **45a**, **45b,** and **45c** are also quite small (1.6, 2.1, and 2.5 kcal/mol, respectively).[55] Apparently **45a** represents the lowest-energy arrangement of $C_{70}$@**42** complex exhibiting the smallest deformation of the clip.

The most important result from the study of $C_{70}$@**42** is that its binding energy is quite similar to that of the $C_{60}$@**42** complex. This is, however, not entirely unexpected since the buckycatcher interacts with roughly a half of both $C_{60}$ and $C_{70}$ surfaces in the inclusion complexes, so π−π stacking interactions should be similar in both cases. The calculated geometries of **42** in both **45a** and $C_{60}$@**42** are very similar, and their degrees of deformation are almost identical, as demonstrated by their calculated $R_d$ distances of 12.78 and 12.80 Å, respectively.[55]

To gain a deeper insight into the origin of the supramolecular binding in the complexes of the buckycatcher, an energy decomposition analysis was performed on $C_{60}$@**42** and $C_{70}$@**42**.[55] This approach separates the contributions to the binding energy of a supramolecule into exchange repulsion ($E_{ER}$), electrostatic ($E_{ES}$), and charge transfer−orbital interaction ($E_{OC}$) energies, which constitute the standard DFT interaction energy ($E_{DFT}$). Addition of the empirical dispersion correction ($E_{disp}$) yields the total interaction energy $E_{tot}$, which differs from the calculated binding energy $\Delta E_b$ by the deformation penalties of both the host and guest molecules. Table 1.2 presents the binding energy decomposition analysis of the buckycatcher complexes with $C_{60}$ and $C_{70}$ performed at the B97-D/TZVP level.[55]

**TABLE 1-2. B97-D/TZVP Binding Energy Decomposition Analysis of $C_{60}$@42 and $C_{60}$@42[a]**

| Compound | $\Delta E_{ER}$ | $\Delta E_{ES}$ | $\Delta E_{OC}$ | $\Delta E_{DFT}$ | $\Delta E_{disp}$ | $\Delta E_{tot}$ |
|---|---|---|---|---|---|---|
| $C_{60}$@**42** | 103.7 | −50.7 | −21.6 | 31.5 | −75.9 | −44.5 |
| $C_{70}$@**42** | 108.9 | −55.4 | −20.6 | 32.9 | −79.7 | −46.8 |

[a]All contributions are given in kilocalories per mole (kcal/mol).

A comparison of the two complexes reveals no difference in the nature of the binding. In both cases the standard DFT contributions are repulsive but are overridden by the strongly attractive dispersion term. The dispersion contribution to binding is slightly larger in $C_{70}$@**42** as a result of a higher number of van der Waals contacts between the carbon atoms of the carbon cage and the corannulene pincers. In line with our original prediction of a "pure" $\pi-\pi$ dispersion character of binding in $C_{70}$@**42**, the energy decomposition analysis classifies both fullerene and buckycatcher supramolecules as typical van der Waals complexes with no specific electrostatic, orbital, or charge transfer interactions.[55] The same conclusion was reached by other authors.[58,59]

***$C_{70}$@42: Experiment.*** Association of the buckycatcher with $C_{70}$ in solution was studied by NMR titration of **42** with $C_{70}$ in toluene-$d_6$ at 293 K.[55] Addition of $C_{70}$ to a solution of **42** causes measurable changes of the chemical shifts of three out of four symmetry-independent protons in the corannulene pincers. Following the procedure described earlier, an association constant of $6800 \pm 400\,M^{-1}$ was estimated. The $K_a$ for $C_{70}$@**42**, although quite high, is lower than the analogous value for $C_{60}$@**42** ($8600 \pm 500\,M^{-1}$). However, both association constants yield very similar free enthalpies of $-5.1$ and $-5.3$ kcal/mol, respectively, proving that the buckycatcher does not exhibit significant specificity in molecular recognition of the two fullerene cages, at least in toluene solutions.

Several batches $C_{70}$@**42** crystals were grown from various solvents, including toluene, $CS_2$, and chlorobenzene. Unfortunately, X-ray crystal structure analysis failed to yield acceptable results, due to crystal defects and/or multiple disorder problems. However, in all cases the presence of 1 : 1 inclusion complexes of $C_{70}$ with buckycatcher was confirmed, along with molecules of the solvents used. Also, in some cases the X-ray data were sufficient to obtain a basic structure of the inclusion complex.[62] As shown in Figure 1-13, the solid-state arrangement of $C_{70}$ inside the

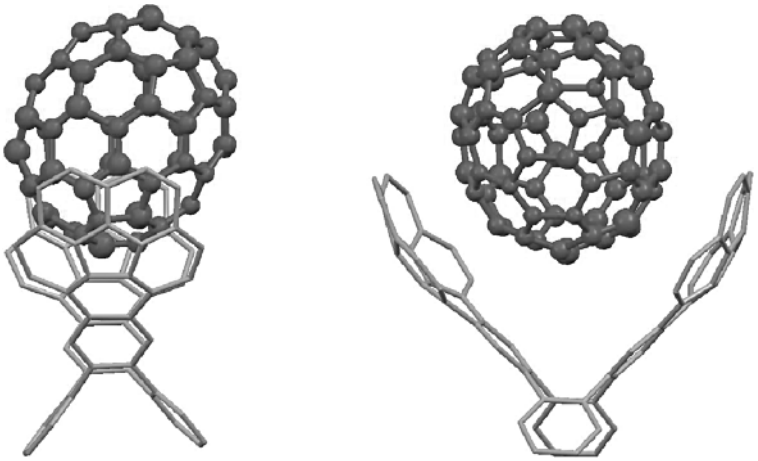

**Figure 1-13.** Two orthogonal views of $C_{70}$@**42***2PhCl in the crystal. The solvating chlorobenzene molecules are omitted for clarity.

cleft of the buckycatcher closely resembles the lowest-energy structure **45a** calculated at the B97-D/TZVP level.

In conclusion, the buckycatcher proved to be an effective molecular receptor for both $C_{60}$ and $C_{70}$ fullerenes in both solution and the solid state. Both inclusion complexes can be described as typical van der Waals complexes bound primarily by London dispersion forces. The existence of the strongly bonded π−π stacked assemblies such as $C_{60}$@**42** and $C_{70}$@**42** proves the importance of π−π stacking of the curved conjugated carbon networks in supramolecular assemblies.

We are currently studying inclusion complexes of the buckycatcher with other guests, including small polar molecules such as trinitrobenzene or DDQ. Several inclusion complexes have been characterized by X-ray crystallography with both *endo*−*endo* (**42a**) and *endo*−*exo* (**42b**) conformations of buckycatcher present. The results of these studies will be published in due course.

### 1-4-4. Potential Clips with Dibenzocyclooctadiene or Dibenzocyclooctatetraene Tethers

A series of highly nonplanar systems with clefts of various sizes and shapes constructed by combining corannulene pincers and cyclooctadiene (COD) or cyclooctatetraene (COT) tethers was synthesized and characterized by X-ray crystal structure determination in our laboratory.[63] The tetrabenzocyclooctatetraene tether present in buckycatcher **42** exhibits some flexibility around its minimum-energy tub-shaped conformation but possesses a high barrier for the tub-to-tub inversion and rather limited conformational space. In contrast, the conformational flexibility of COD or COT tethers allows for an adoption of conformations unavailable for the buckycatcher.

Again, the syntheses utilized isocorannulenofuran (**23**) and 2-trimethylsilylcorannulenyltrifluoromethanesulfonate (**28**, a precursor for 1,2-didehydrocorannulene) as synthons (Scheme 1-14).

Synthesis of **46**, a molecular clip with a COT tether and corannulene and benzene pincers, was achieved by a Diels−Alder reaction of **23** with benzocyclobutadiene, generated *in situ* from dibromide **47**, which leads to the formation of two isomeric adducts, *endo*-**48** and *exo*-**48** (∼9 : 1). The major adduct was characterized by X-ray crystallography (Figure 1-14), showing a highly nonplanar "closed clam" structure, with the benzene ring of the benzocyclobutane moiety located over the convex side of the corannulene unit. Not surprisingly, a significant shielding of the four hydrogen atoms of the AA′BB′ system of the benzene ring was

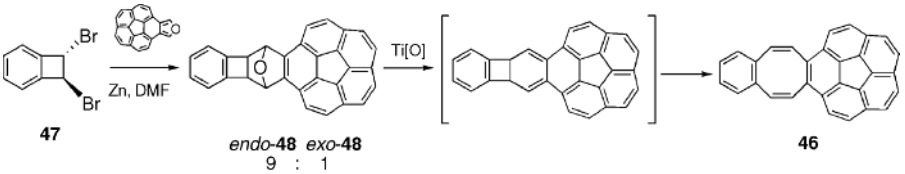


**Scheme 1-14.** Synthesis of **46**.

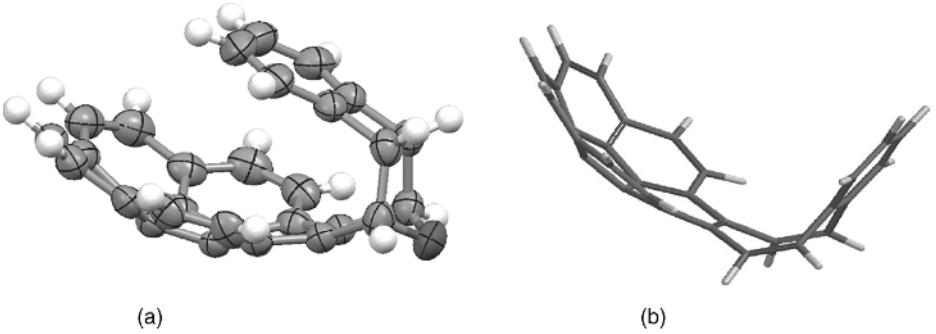


**Figure 1-14.** (a) Crystal structure of *endo*-**48;** (b) MM2-optimized structure of **46**.

observed with their chemical shifts appearing in the $^1$H NMR spectrum as broad multiplets centered at 5.4 and 5.9 ppm, significantly upfield from the usual chemical shift of aromatic protons. In contrast, the analogous protons in *exo*-**48** appear as sharp AA'BB' multiplets centered in the usual range (7.2 and 7.3 ppm).

*Exo*-**48** and *endo*-**48** were deoxygenated with low-valence titanium to form $C_{30}H_{16}$ hydrocarbon **46**, presumably through the dihydrobiphenylene intermediate (Scheme 1-14). The target **46** was not characterized by X-ray crystallography but is expected to adopt an "open-clam" conformation of a clip, with corannulene and benzene pincers located on the tub-shaped COT tether (Figure 1-14).[63]

Molecular clips with more flexible 1,5-COD subunits were also synthesized (Scheme 1-15).[63]

Again, isofuran (**23**) reacted with an excess of the reactive alkyne generated by dehydrobromination of a mixture of dibromocyclooctadienes, producing a mixture of two major adducts, **49** and **50**. X-ray crystal structure determination of **49** shows an interesting and rather unusual arrangement of the cyclooctadiene ring in which six carbon atoms are almost coplanar and lie in a plane approximately perpendicular

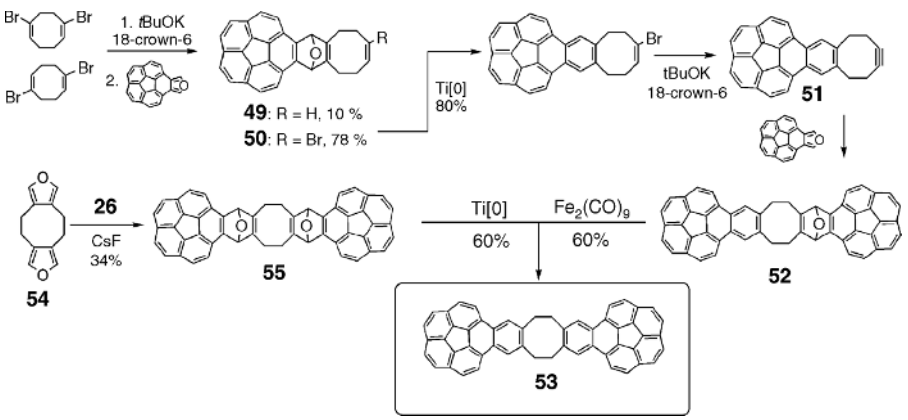


**Scheme 1-15.** Two alternative synthetic routes to **53**.

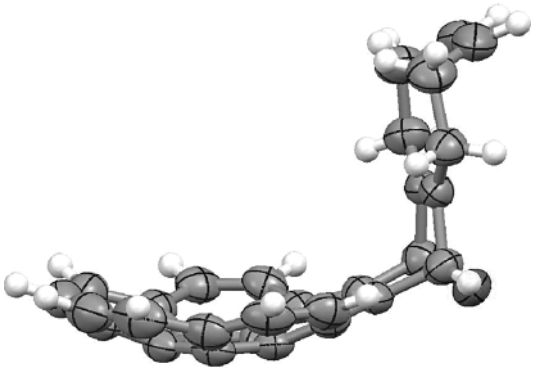

**Figure 1-15.** Crystal structure of the adduct **49**.

to the average plane of the corannulene subunit in an open-clam arrangement (Figure 1-15).

Endoxide (**50**) was deoxygenated and later dehydrobrominated to the reactive dienophile **51**. Diels–Alder cycloaddition of **51** to isofuran **23** lead to endoxide **52**, which, in turn, was deoxygenated with diiron nonacarbonyl to bis(benzocorannulene) cyclooctadiene (**53**), a $C_{52}H_{28}$ molecular clip with a COD tether and two benzocorannulene pincers.[63]

An alternative synthetic route to **53** utilizes the 1,2-didehydrocorannulene precursor **28** and difuran **54**, synthesized in one step from commercially available dipropargyl ether.[64] A double-Diels–Alder cycloaddition yields a mixture of two isomeric products, presumably *syn*- and *anti*-**55**, which were reduced with low-valence titanium to produce **53** in a moderate yield of ~60%.[63]

The $C_{52}H_{28}$ hydrocarbon (**53**) represents a more flexible version of buckycatcher with a COD tether and two benzocorannulene pincers. We have studied its conformational preferences by both MM2 and DFT calculations in comparison with the simpler analog of **53**, 5,6,11,12-tetrahydrodibenzo[*a,e*]cyclooctene (**56**). The conformational space of **56** was previously thoroughly studied by both computational and experimental methods.[65] Three conformers of **56** were located: twist–boat (**56TB**), chair (**56C**) and twist (**56T**) (Figure 1-16). Low-temperature NMR studies reveal the

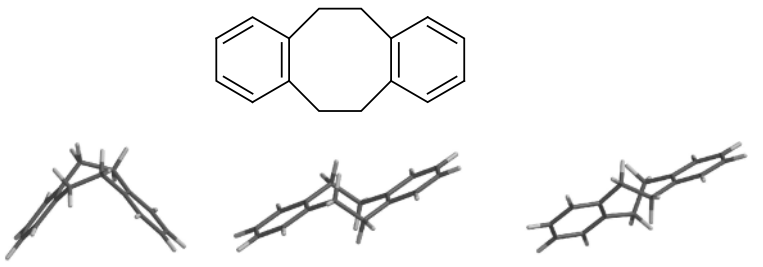


**Figure 1-16.** Three conformations of 5,6,11,12-tetrahydrodibenzo[*a,e*]cyclooctene.

| | TB | C | T |
|---|---|---|---|
| **53** | 0.00 | 8.16 | 11.43 |
| **56** | 0.00 | 0.24 | 3.47 |

**Figure 1-17.** B97-D/TZVP calculated minimum-energy conformations of **53** and the relative energies (kcal/mol) of the twist–boat (**TB**), chair (**C**), and twist (**T**) conformers of **53** and **55**.

existence of two conformers, namely, **56TB** and **56C,** in comparable amounts. Accordingly, theoretical studies predicted the energies of the two conformers to be quite similar, with the twist **56T** conformer having significantly higher energy, which precludes its detection by NMR experiments. By analogy to the model system, three conformers of **53** were also considered and optimized at the B97-D/TZVP level. Their geometries and relative energies are presented in Figure 1-17. Relative energies of the three corresponding conformers of the dibenzo analog **56** calculated at the same level of theory are also shown in Figure 1-17 for comparison.[63]

In contrast to **56**, twist–boat conformer of **53** is calculated to be very strongly favored over the remaining **53C** and **53T** by over 8 kcal/mol. The strong preference for **53TB** is also predicted by MM calculations. The presence of the large benzocorannulene pincers located on a flexible cyclooctadiene tether causes a strongly stabilizing intramolecular π–π stacking interaction in the **TB** conformation. The two pincers in **53TB** are clearly arranged to maximize van der Waals attraction with the shortest nonbonding carbon–carbon distances between 3.44 and 3.94 Å.

It has been observed that **53** has a very limited solubility in organic solvents, in contrast to other corannulene-based molecular clips.[63] Its solubility is significantly lower than that of the larger and less flexible buckycatcher **42**. The strong gas-phase preference for the internally π–π stacked **TB** conformation may explain the low solubility of **53** since the solvent-accessible surface of this conformation is dramatically reduced in comparison to the usual "open" conformations of other buckybowls. There is no doubt that **53TB** should prevail in the gas phase or in weakly solvating solvents. Unfortunately, because of the aforementioned low solubility of **53,** low-temperature NMR studies were not attempted. On the other hand, in the presence of strongly solvating solvents the open conformer **53C** may become preferred. Indeed, X-ray crystal structure determination of a 1 : 1 solvate of **53** with nitrobenzene revels that the chair conformation prevails in the solid state of the solvate (Figure 1-18).[63] The disordered nitrobenzene molecule is encapsulated by two neighboring molecules of **53** and is in van der Waals contacts with the concave sides of the benzocorannulene pincers.

### 1-4-5. Tweezers in a Haystack: Molecular Mechanics as a Screening Tool

Future research will seek to synthesize molecular clips and tweezers that will selectively complex fullerenes and other guest molecules. The classic approach,

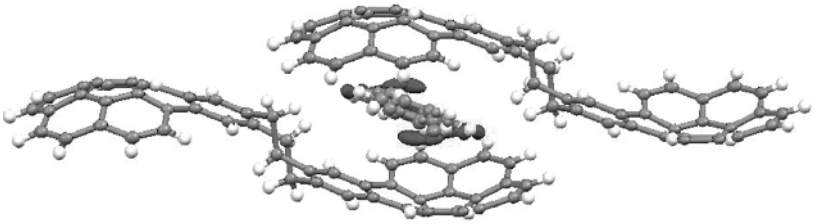

**Figure 1-18.** Crystal structure of **53**$^{*}$$PhNO_2$ solvate. Several overlapping orientations of the disordered molecules of $PhNO_2$ are shown. The second molecule of **53** is added to demonstrate the encapsulation of nitrobenzene.

which includes (1) selecting tethers and pincers that appear likely to maximize binding of the target guests (fullerenes) with the host, (2) synthesizing numerous molecular clips and tweezers, and then (3) testing their molecular recognition abilities in solution (by spectroscopic titration experiments) and in the solid state (by X-ray crystallography), is a lengthy, tedious, and expensive venture. The rational design of molecular clips and tweezers with desired properties hinges on computational methods capable of calculating supramolecular assembly binding energies with reasonable accuracy.

As we have noted earlier, the new DFT methods with dispersion interactions are capable of reasonable accuracy. Unfortunately, these calculations for large supramolecular assemblies are still quite time-consuming. The even more time-demanding MP2, coupled-cluster or related highly electron-correlated methods, are prohibitively expensive for the large supramolecular systems we plan to synthesize.

We therefore have explored molecular mechanics (MM) methods for a crude but fast screening of the ability to form complexes between the pool of potential molecular clips and tweezers and guest molecules. MM methods suffer from several limitations and drawbacks, but at least they recognize van der Waals nonbonding attractions. Our strategy is to compare the MM results for a series of similar host–guest assemblies to provide useful information about trends rather than supply exact binding energies. To illustrate this approach, we show below the MM2-calculated binding energies of the supramolecular complexes of $C_{60}$ with some molecular clips equipped with corannulene pincers (Figure 1-19).

The MM2-calculated binding energies of the supramolecular dimers studied vary from 19.4 to 25.7 kcal/mol. We can assess these numbers by comparing the experimentally determined association behavior of some of the molecular clips described earlier. Thus, **34** and its simpler analog **57**, both synthesized in our laboratory, failed to exhibit any significant association with $C_{60}$ in solutions, while buckycatcher **42** forms a strong inclusion complex in both solid state and toluene solutions. The difference in their complexing abilities is reflected in the calculated binding energies, predicted to be stronger for $C_{60}$@**42** by $\sim$5 kcal/mol than in $C_{60}$@**34**. According to these data, **59** is not a strong candidate for an effective receptor for buckminsterfullerene, whereas **58** may show promise. Interestingly, **60**, an unknown analog of **34** that is augmented with two additional benzene rings, may

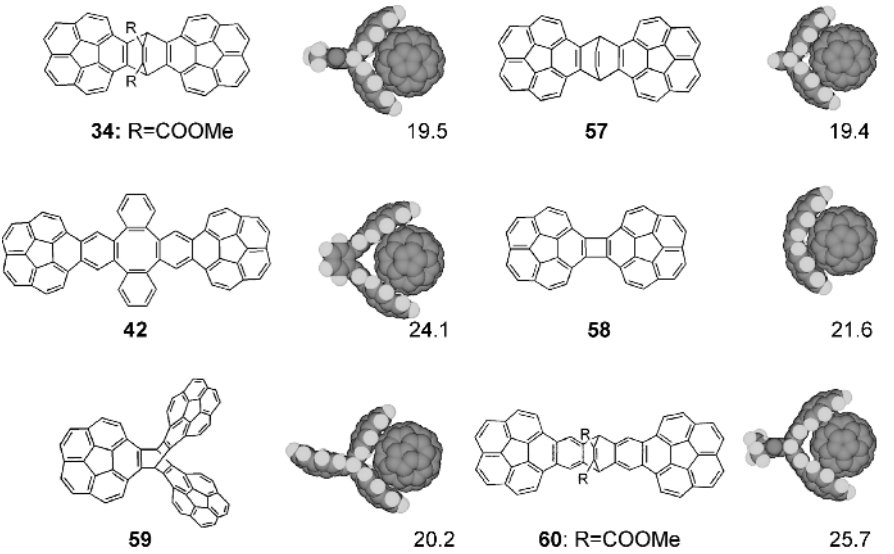


**Figure 1-19.** MM2 structures and binding energies (kcal/mol) of the inclusion complexes of $C_{60}$ with various molecular clips.

be an even better acceptor of $C_{60}$ than buckycatcher **42**. Its binding to $C_{60}$ is predicted to be 1.6 kcal/mol stronger than **42**, and if the MM2 prediction is correct, **60** may exhibit an association constant for complex formation an order of magnitude higher than **34**.

The physical basis for relying on trends in the binding energies is simple. The binding energy is calculated as the energy difference between product and substrate and relates to $\Delta H^\circ$ of the complex formation in the gas phase. As we discussed earlier, two other factors also affect the free energy of association ($\Delta G^\circ$) in solution: the entropy and the solvation effects. Both these factors work against the supramolecular assembly formation but should be similar in a series of related assemblies. Therefore, the larger the binding energy of a supramolecular assembly, the more likely the complex will be observed in condensed phases.

The focus on trends and not individual binding energies opens the door to freedom from only one MM method. Although the binding energies of the supramolecular complexes of $C_{60}$ with our molecular clips calculated with other force fields are quite different from those calculated using MM2, the trends are very similar. For example, Amber 96 calculations give binding energies of 32.1, 37.3, and 39.5 kcal/mol for $C_{60}$@**34**, $C_{60}$@**42**, and $C_{60}$@**60**, respectively, which are significantly higher than the MM2 results. However, the *relative* binding energies of these three supramolecular complexes are very similar with both force fields. Therefore, we conclude that MM should be a useful tool for rapid screening for the best synthetic targets if trends, not the individual binding energies, are examined and compared with available experimental data.

## 1-5. IF YOU BUILD IT, WHAT'S THE USE?

We now possess the synthetic methodology to construct novel molecular clips and tweezers with bowl-shaped pincers. The progress we have detailed in the practical production of these compounds allows for investigation of their properties and for consideration of their possible applications. So what possible uses could buckycatchers have?

Predicting the future uses of any new technology is often an exercise in futility and embarrassment. However, two major uses of buckycatchers that we envision are as stationary phases in liquid chromatography for the separation of fullerenes and as buckycatcher–fullerene complexes in photovoltaic devices.

Fullerenes can now be produced in multiton quantities and are being commercialized in numerous medicinal and industrial applications. There is no agreement on fullerenes as an occupational hazard or ultimately as a consumer or environmental hazard, but more recent studies prove that fullerenes and their derivatives pose potential health risks.[66] The need for chromatographic separation of fullerenes and detection at low concentration will assuredly grow in the coming years.

We have proved that molecular clips and tweezers with buckybowl pincers interact with fullerenes through π–π convex–concave stacking of the curved carbon networks. These clips can be attached to stationary chromatographic phases and will modify the absorption of fullerenes onto the surface and change their elution times. We envision buckycatchers, engineered for specificity, immobilized on silica gel or other porous stationary phases for the separation of fullerene mixtures.

The second major use of buckycatchers is in molecular electronics, specifically photovoltaic devices. The fullerene-hosting abilities of our molecular clips should enable deposition of the guest (fullerene) cages onto a surface if a monolayer of the host buckycatchers can be generated on a solid support. The molecular clips with polar anchors such as **60** (or its dicarboxy analog) are good candidates for successful deposition onto the surface of a conducting support. Once the host monolayer is formed, it will be exposed to a solution of fullerene and, after solvent removal, a double host–guest layer will be formed on the solid support surface (Figure 1-20).

These bilayers are potential light acceptors for photovoltaic devices. Fullerenes and their derivatives have been widely employed in photovoltaic devices since they absorb light very efficiently and, in addition, they are good electron acceptors. Not

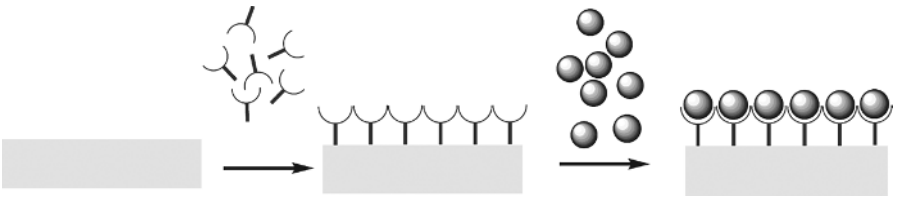

**Figure 1-20.** A cartoon representation of a bilayer formation on a solid support.

surprisingly, our $C_{60}$@**42** has already been studied theoretically for possible charge transfer mediation.[67] This study predicts that the hole transfer from fullerene to another fullerene mediated by **42** is three orders of magnitude faster than the analogous excess electron transfer. Another theoretical study predicts a possibility of a significant modulation of the two-photon absorption (TPA) process in $C_{60}$@**42**, thus making it possible to apply these inclusion complexes as TPA active materials.[68]

Other possible uses of buckycatchers include hydrogen storage materials and novel transition metal ligands. Likely, the most important uses of buckycatchers have yet to be imagined. While the future may be uncertain, the long journey to buckycatchers illustrates the sometimes frustrating but ultimately satisfying pursuit of novel organic molecules.

## ACKNOWLEDGMENTS

Support to AS from the Chemical Sciences, Geosciences and Biosciences Division, Office of Basic Energy Sciences, Office of Science, US Department of Energy through Grant DE-FG02-04ER15514 is greatly appreciated. We thank all the students and research associates for their contributions to this project. AS acknowledges a long and fruitful collaboration with Professor Peter W. Rabideau in the area of novel PAHs.

## REFERENCES

1. C.-W. Chen, H. W. Whitlock, Jr., *J. Am. Chem. Soc.* **1978**, *100*, 4921–4922.
2. (a) M. Havlik, V. Král, R. Kaplánek, B. Dolenský, *Org. Lett.* **2008**, *10*, 4767–4769; (b) S. C. Zimmerman, *Top. Curr. Chem.* **1993**, *165*, 71–102.
3. (a) B. Branchi, V. Balzani, P. Ceroni, M. C. Kuchenbrandt, F.-G. Klärner, D. Bläser, R. Boese, *J. Org. Chem.* **2008**, *73*, 5839–5851; (b) P. Polavarapu, H. Melander, V. Langer, A. Gogoll, H. Grennberg, *New J. Chem.* **2008**, *32*, 643–651; (c) R. P. Sijbesma, R. J. M. Nolte, *Top. Curr. Chem.* **1995** *175*, 25–56.
4. (a) M. Skibiński, R. Gómez, E. Lork, V. A. Azov, *Tetrahedron* **2009**, *65*, 10348–10354; (b) T. Nishiuchi, Y. Kuwatani, T. Nishinaga, M. Iyoda, M. *Chem. Eur. J.* **2009**, *15*, 6838–6847.
5. M. Harmata, *Acc. Chem. Res.* **2004**, *37*, 862–873.
6. R. A. Pascal, Jr. *Chem. Rev.* **2006**, *106*, 4809–4819.
7. J. Lu, D. M. Ho, N. J. Vogelaar, C. M. Kraml, R. A. Pascal, Jr., *J. Am. Chem. Soc.* **2004**, *126*, 11168–11169.
8. (a) W. E. Barth, R. G. Lawton, *J. Am. Chem. Soc.* **1966**, *88*, 380–381; (b) W. E. Barth, R. G. Lawton, R. G. *J. Am. Chem. Soc.* **1971**, *93*, 1730–1745.
9. (a) H. W. Kroto, J. R. Heath, S. C. O'Brien, R. F. Curl, R. E. Smalley, *Nature* **1985**, *318*, 162–163; (b) K. M. Kadish, R. S. Rouff (eds.), *Fullerenes: Chemistry, Physics and Technology*, Wiley, New York, 2000.
10. (a) Y.-T. Wu, J. S. Siegel, *Chem. Rev.* **2006**, *106*, 4843–4867; (b) V. M. Tsefrikas, L. T. Scott, *Chem. Rev.* **2006**, *106*, 4868–4884; (c) A. Sygula, P. W. Rabideau, *Carbon Rich*

*Compounds*, M. M. Haley, R. R. Tykwinski, (eds.), Wiley-VCH, Weinheim, 2006, pp. 529–565.

11. J. M. Hermida-Ramón, M. Mandado, M. Sánchez-Lozano, C. M Estévez, *Phys. Chem. Chem. Phys.* **2010**, *12*, 164–169.
12. (a) M. O. Sinnokrot, C. D. Sherrill, *J. Phys. Chem. A* **2006**, *110*, 10656–10668; (b) E. C. Lee, D. Kim, P. Jurecka, P. Tarakeshwar, P. Hobza, K. S. Kim, *J. Phys. Chem. A* **2007**, *111*, 3446–3457; (c) T. Janowski, P. Pulay, *Chem. Phys. Lett.* **2007**, *447*, 27–32.
13. T. F. Headen, C. A. Howard, N. T. Skipper, M. A. Wilkinson, D. T. Bowron, A. K. Soper, *J. Am. Chem. Soc.* **2010**, *132*, 5735–5742.
14. (a) J. C. Hanson, C. E. Nordman, *Acta Cryst. B* **1976**, *B32*, 1147–1153; (b) M. A. Petrukhina, K. W. Andreini, J. Mack, L. T. Scott, *J. Org. Chem.* **2005**, *70*, 5713–5716.
15. A. Sygula, H. E. Folsom, R. Sygula, A. H. Abdourazak, Z. Marcinow, F. R. Fronczek, P. W. Rabideau, *Chem. Commun.* **1994**, 2571–2572.
16. H. Becker, G. Javahery, S. Petrie, P.-C. Chemg, H. Schwarz, L. T. Scott, D. K. Bohme, *J. Am. Chem. Soc.* **1993**, *115*, 11636–11637.
17. (a) S. Mizyed, P. E. Georghiou, M. Bancu, B. Cuadra, A. K. Rai, P. Cheng, L. T. Scott, *J. Am. Chem. Soc.* **2001**, *123*, 12770–12774; (b) P. E. Georghiou, A. H. Tran, S. Mizyed, M. Bancu, L. T. Scott, *J. Org. Chem.* **2005**, *70*, 6158–6163.
18. T. Kawase, H. Kurata, *Chem. Rev.* **2006**, *106*, 5250–5273.
19. A. Sygula, F. R. Fronczek, R. Sygula, P. W. Rabideau, M. M. Olmstead, *J. Am. Chem. Soc.* **2007**, *129*, 3842–3843.
20. W. Xiao, D. Passerone, P. Ruffieux, K. Aït-Mansour, O. Gröning, E. Tosatti, J. S. Siegel, R. Fasel, *J. Am. Chem. Soc.* **2008**, *130*, 4767–4771.
21. S. Kristyán, P. Pulay, *J. Chem. Phys. Lett.* **1994**, *229*, 175–180.
22. E. R. Johnson, G. A. DiLabio, *J. Chem. Phys. Lett.* **2006**, *419*, 333–339.
23. V. R. Cooper, L. Kong, D. C. Langreth, *Phys. Procedia* **2010**, *3*, 1417–1430.
24. E. R. Johnson, I. D. Mackie, G. A. DiLabio, *J. Phys. Org. Chem.* **2009**, *22*, 1127–1135.
25. (a) S. Grimme, *J. Comput. Chem.* **2006**, *27*, 1787–1799; (b) S. Grimme, J. Antony, T. Schwabe, C. Mück-Lichtenfeld, *Org. Biomol. Chem.* **2007**, *5*, 741–758.
26. Á. Vázquez-Mayagoitia, C. D. Sherrill, E. Aprà, B. G. Sumpter, *J. Chem. Theory Comput.* **2010**, *6*, 727–734.
27. (a)Y. Zhao, D. G. Truhlar, *Acc. Chem. Res.* **2008**, *41*, 157–167; (b) Y. Zhao, D. G. Truhlar, *Theor. Chem. Acc.* **2008**, *120*, 215–241.
28. S. Tsuzuki, T. Uchimaru, K. Tanabe, *J. Phys. Chem. A* **1998**, *102*, 740–743.
29. R. Peverati, K. K. Baldridge, *J. Chem. Theory Comput.* **2008**, *4*, 2030–2048.
30. A. Sygula, S. Saebø, *J. Int. Quant. Chem.* **2009**, *109*, 65–72.
31. (a) J. T. Craig, M. D. W. Robins, Aust. *J. Chem.* **1968**, *21*, 2237–2245; (b) R. H. Jacobson, PhD dissertation, Univ. California, Los Angeles, **1986**; (c) J. R. Davy, M. N. Iskander, J. A. Reiss, *Tetrahedron Lett*. **1978**, 4085–4088.
32. L. T. Scott, M. M. Hashemi, D. T. Meyer, H. B. Warren, *J. Am. Chem. Soc.* **1991**, *113*, 7082–7084.
33. L. T. Scott, P.-C. Cheng, M. M. Hashemi, M. S. Bratcher, D. T. Meyer, H. B. Warren, *J. Am. Chem. Soc.* **1997**, *119*, 10963–10968.

34. (a) A. H. Abdourazak, A. Sygula, P. W. Rabideau, *J. Am. Chem. Soc.* **1993**, *115*, 3010–3011; (b) A. Sygula, A. H. Abdourazak, P. W. Rabideau, *J. Am. Chem. Soc.* **1996**, *118*, 339–343.
35. (a) P. W. Rabideau, A. H. Abdourazak, H. E. Folsom, Z. Marcinow, A. Sygula, R. Sygula, *J. Am. Chem. Soc.* **1994**, *116*, 7891–7892; (b) A. H. Abdourazak, A. Z. Marcinow, A. Sygula, R. Sygula, P. W. Rabideau, *J. Am. Chem. Soc.* **1995**, *117*, 6410–6411.
36. (a) L. T. Scott, *Angew. Chem. Int. Ed.* **2004**, *43*, 4994–5007; (b) L. T. Scott, M. S. Bratcher, S. Hagen, *J. Am. Chem. Soc.* **1996**, *118*, 8743–8744.
37. L. T. Scott, M. M. Boorum, B. J. McMahon, S. Hagen, J. Mack, J. Blank, H. Wegner, A. de Meijere, *Science* **2002**, *295*, 1500–1503.
38. (a) T. J. Seiders, K. K. Baldridge, J. S. Siegel, *J. Am. Chem. Soc.* **1996**, *118*, 2754–2755; (b) A. Borchardt, K. Hardcastle, P. Gantzel, J. S. Siegel, *Tetrahedron Lett*. **1993**, *34*, 273–276.
39. J. E. McMurry, *Chem. Rev.* **1989**, *89*, 1513–1524 and references cited therein.
40. G. A. Olah, G. K. S. Prakash, *Synthesis* **1976**, 607–609.
41. A. Sygula, P. W. Rabideau, *J. Am. Chem. Soc.* **1998**, *120*, 12666–12667.
42. A. Sygula, P. W. Rabideau, *J. Am. Chem. Soc.* **1999**, *121*, 7800–7803.
43. (a) T. J. Seiders, K. K. Baldridge, E. L. Elliott, G. H. Grube, J. S. Siegel, *J. Am. Chem. Soc.* **1999**, *121*, 7439–7440; (b) T. J. Seiders, E. L. Elliott, G. H. Grube, J. S. Siegel, *J. Am. Chem. Soc.* **1999**, *121*, 7804–7813.
44. A. Sygula, P. W. Rabideau, *J. Am. Chem. Soc.* **2000**, *122*, 6323–6324.
45. P. Bachavala, M. S. Thesis, Mississippi State Univ., Mississippi State, **2006**.
46. (a) A. Sygula, G. Xu, Z. Marcinow, P. W. Rabideau, *Tetrahedron* **2001**, *57*, 3637–3644; (b) G. Xu, A. Sygula, Z. Marcinow, P. W. Rabideau, *Tetrahedron Lett*. **2000**, *41*, 9931–9934.
47. A. Sygula, S. D. Karlen, R. Sygula, P. W. Rabideau, *Org. Lett.* **2002**, *4*, 3135–3137.
48. A. Sygula, F. R. Fronczek, P. W. Rabideau, *Tetrahedron Lett*. **1997**, *38*, 5095–5098.
49. A. Sygula, R. Sygula, P. W. Rabideau, *Org. Lett.* **2005**, *7*, 4999–5001.
50. A. Sygula, R. Sygula, L. Kobryn, *Org. Lett.* **2008**, *10*, 3927–3930.
51. (a) Y. Himeshima, T. Sonoda, H. Kobayashi, *Chem. Lett*. **1983**, 1211–1214; (b) D. Peña, A. Cobas, D. Pérez, E. Guitián, *Synthesis* **2002**, 1454–1458.
52. A. Sygula, R. Sygula, P. W. Rabideau, *Org. Lett.* **2006**, *8*, 5909–5911.
53. A. Sygula, R. Sygula, A. Ellern, P. W. Rabideau, *Org. Lett.* **2003**, *5*, 2595–2597.
54. (a) S. M. Bacharach, *J. Org. Chem.* **2009**, *74*, 3609–3611 and references cited therein; (b) H. Huang, T. Stewart, M. Gutmann, T. Ohhara, N. Niimura, Y.-X. Li, J.-F. Wen, R. Bau, H. N. C. Wong, *J. Org. Chem.* **2009**, *74*, 359–369 and references cited therein.
55. C. Mück-Lichtenfeld, S. Grimme, L. Kobryn, A. Sygula, *Phys. Chem. Chem. Phys.* **2010**, *12*, 7091–7097.
56. S. Grimme, C. Mück-Lichtenfeld, J. Antony, *J. Phys. Chem. C* **2007**, *111*, 11199–11207.
57. M. Makha, A. Purich, C. L. Raston, A. N. Sobolev, *Eur. J. Inorg. Chem.* **2006**, 507–517.
58. Y. Zhao, D. G. Truhlar, *Phys. Chem. Chem. Phys.* **2008**, *10*, 2813–2818.
59. B. M. Wong, *J. Comput. Chem.* **2009**, *30*, 51–56.
60. (a) C. D. Sherrill, T. Takatani, E. G. Hohenstein, *J. Phys. Chem. A* **2009**, *113*, 10146–10159; (b) K. E. Riley, M. Pitonak, J. Cerny, P. Hobza, *J. Chem. Theory Comput.* **2010**, *6*, 66–80.

61. (a) P. Hobza, H. L. Selzle, E. W. Schlag, *J. Phys. Chem.* **1996**, *100*, 18790–18794; (b) V. Špirko, O. Enkvist, P. Soldan, H. L. Selzle, E. W. Schlag, P. Hobza, *J. Chem. Phys.* **1999**, *111*, 572–582.

62. F. R. Fronczek, A. Sygula, unpublished results.

63. L. Kobryn, W. P. Henry, F. R. Fronczek, R. Sygula, A. Sygula, *Tetrahedron Lett*. **2009**, *50*, 7124–7127.

64. H. Detert, B. Rose, W. Mayer, H. Meier, *Chem. Ber.* **1994**, *127*, 1529–1532.

65. M. L. Jimeno, I. Alkorta, J. Elguero, J. E. Anderson, R. M. Claramunt, R. M. Lavandera, *New J. Chem.* **1998**, *22*, 1079–1083 and references therein.

66. (a) J. Gao, H. L. Wang, A. Shreve, R. Iyer, *Toxicol. Appl. Pharmacol.* **2010**, *244*, 130–143; (b) E.-J. Park, H. Kim, Y. Kim, J. Yi, K. Choi, K. Park, *Toxicol. Appl. Pharmacol.* **2010**, *244*, 226–233.

67. A. A. Voityuk, M. Duran, *J. Phys. Chem. C* **2008**, *112*, 1672–1678.

68. S. Chakrabarti, K. Ruud, *J. Phys. Chem. A* **2009**, *113*, 5485–5488.